



Particle squeezing in narrow confinements

Zhifeng Zhang¹ · Jie Xu² · Corina Drapaca¹

Received: 5 June 2018 / Accepted: 18 September 2018
© Springer-Verlag GmbH Germany, part of Springer Nature 2018

Abstract

Many lab-on-a-chip applications require processing of droplets, cells, and particles using narrow confinements. The physics governing the process of a particle squeezing through narrow confinement is complex. Various models and applications have been developed in this area in recent years. In the present paper, we review the physics, modeling approaches, and designs of narrow confinements for the control of deformable droplets, cells, and particles. This review highlights the interdisciplinary nature of the problem, since the experimental, analytical, and numerical methods used in studies of particle squeezing through narrow confinements come from various fields of science and technology.

Keywords Droplets · Cells · Particles · Narrow confinements · Soft matter · Chip design · Fluid mechanics · Chemical engineering

1 Introduction

Deformable particles that are dispersed in a carrier liquid and confined in a microspace are widely investigated in various contexts of interest to many industries. These particles include soft liquid/solid/viscoelastic particles and complex particles like biological cells. When designing a multiphase lab-on-a-chip device, many considerations are needed, such as mass transfer between phases, deformation of the interface, and accurate manipulation of the dispersed phases, i.e., particles. Narrow confinements are often used to achieve specific design goals and the dispersed phases, or particles, are often forced into the narrow confinements for various purposes. As a result, the physical model of squeezing a particle through a constricted confinement (or “the model” hereafter) has become more and more popular in a variety of applications (Benet et al. 2017; Beresnev et al. 2011), such as geophysical engineering, chemical engineering, water resource research, food industry, oil/gas industry,

and lab-on-a-chip devices. Moreover, in many applications that involve membranes, filters, and packed beds, the basic functional units are constricted pores, which are narrow confinements *per se*, and microparticles usually need to be either forced through or get blocked at these confinements. Furthermore, cells or tissue under small confinements is relevant to many applications such as pathology studies, precision medicine, bio-printing, and microfluidic devices design.

In general, the use of narrow confinements for particle squeezing at microscale has the following advantages:

1. Simplicity.

For example, although AFM (Atomic Force Microscope) can accurately measure the properties of cells or tissue, the micropipette aspiration method utilizing the tip of the pipette as a narrow confinement for the cells is still widely used for cell mechanical property measurements due to its simple setup and easy operations during measurements.

2. Low manufacture cost.

The manufacture of a narrow confinement at microscale is usually straightforward, making mass production feasible.

3. Reliability.

Many advanced particle-handling tools like optic and acoustic tweezers are complex and prone to be unstable. On the contrary, a narrow confinement has no moving

✉ Zhifeng Zhang
zfzhang@psu.edu; alex.zfzhang@gmail.com

✉ Corina Drapaca
csd12@psu.edu

¹ Engineering Science and Mechanics, The Pennsylvania State University, State College, PA 16802, USA

² Department of Mechanical and Industrial Engineering, University of Illinois at Chicago, Chicago, IL 60607, USA

parts and requires no unique energy sources making it very reliable for repeatable experiments.

In this paper, we review many aspects of the particle-squeezing problem and the theoretical, experimental, and numerical tools used to tackle this problem. The focus of the review is on the design of narrow-confinement channels for different types of particles in various application contexts. After a general review of the theoretical background and numerical models, a summary of emerging applications is provided, followed by a detailed discussion on confinement design and particle influence. The mechanics (Herant et al. 2005), kinematics (Drury and Dembo 1999), fluid dynamics (Zhang et al. 2015), and deformation dynamics (Legait 1983; Legait et al. 1983) of the particles are also discussed. We do not review particle-laden flow in a channel without any sudden constriction, nor do we cover pure fluid mechanics in a constriction without particles. Although gas bubbles have various applications, we do not review them here. This review should be of interest to chemical/petroleum engineers, biologists, and fluid dynamists working on the design of narrow confinements.

2 Theoretical background and numerical models

The model that describes the motion of deformable particles squeezed through a narrow confinement has two aspects that deserve consideration: the narrow confinement itself and the particles in the flow. The detailed review of these two aspects is provided in later sections.

2.1 Model description

Assuming a deformable particle moves through a constricted channel from left to right, a comparison of different confinement possibilities is shown in Fig. 1. If D is the size of the confinement and d is the diameter of the particle, then D/d is called the confinement ratio. When $D/d=0$, the particle collides with a solid wall. Important applications of this model include thermal spray and surface coating. The regime where $0 < D/d < 1$ is the focus of this review, since most relevant lab-on-a-chip applications fall in this regime. For example, $D/d < 0.7$ has been used to simulate neutrophils

pulmonary microcirculation (Shirai and Masuda 2013) and $D/d=0.1$ has been used in hydrogel tests (Hendrickson and Lyon 2010). More applications can be seen in the following section, “Summary of applications”. In this regime, the deformation of the particles especially droplets mainly depends on the capillary number (Kadivar and Farrokhbin 2017). However, we exclude from our discussion the cases when D/d is much smaller than 1 (close to 0), in which the particle is under extreme confinement and very difficult to be squeezed into the confinement. Relevant applications (D/d close to 0) include lipid bilayer properties measurement and ink penetration into paper. The confinement of ratio $D/d=1$ is commonly used in precise mechanical structures such as rollers in a bearing or bullet in a muzzle. For a weak confinement at $D/d > 1$, many applications such as cells under shear flow in blood vessel (Lazaro et al. 2014) and chemical processing have been widely studied. As reported, the deformation of a particle is strongly affected by D/d and the position of the particle in the channel in this regime. Multiple particles flowing through a narrow confinement were concluded as a probability problem (To et al. 2015), which is also outside the scope of the present review.

2.2 Numerical techniques

In numerical simulations of a particle squeezing through a narrow confinement, interface tracking is one key component. The direct contact of the particle and the confinement wall induces high stress, which is numerically challenging. Usually, algorithms are high resolutions (Zinchenko and Davis 2017) or high cost (Kan et al. 1998). Summaries and comparisons of numerical methods implemented in commercially available and open-sourced software that have been used in simulating a particle squeezing through a narrow confinement are given in Table 1. Some other potential approaches by the multiphase flow simulation can be found in a recent comprehensive review (Wörner 2012).

The methods on top rows of Table 1, such as Volume of Fluid, level set, and phase field, made considerable assumptions to simplify the simulation. Therefore, these methods can usually provide quicker solutions. As a result, the results may have limitations such as lacking strict mass conservation. To makeup, Ansys Fluent provides a coupled level set-VOF method, which provides better mass convergence and accurate curvature. Ansys Fluent performs

Fig. 1 Confinement ratio. The blue lines represent the walls of a solid channel situated distance D apart, and the green circle represents a particle. By definition, D/d is the confinement ratio. (Color figure online)

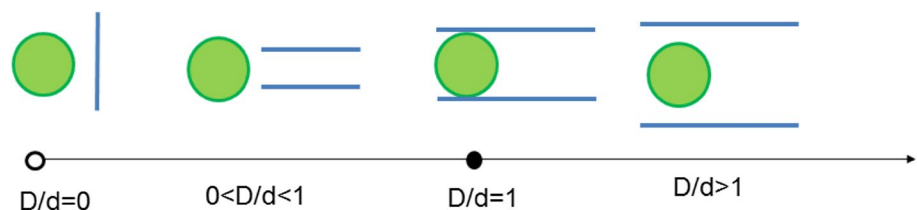


Table 1 Numerical algorithms/techniques used in simulating particle squeezing through a narrow confinement compared by order of availability and computational cost

Numerical algorithm		Comments	References
Volume of fluids ^a	Capability	Droplet model, Newtonian, and simple Non-Newtonian fluid	Darvishzadeh and Priezjev (2012) Zhang et al. (2014)
	Advantage ^a	ANSYS Fluent; Quick solution	Zhang et al. (2018)
	Disadvantage	Fluid model only, no solid; lack of strict mass conservation	
Level- set ^a	Capability	Cerebrospinal Fluid Sampling	Christafakis and Tsangaris (2008)
	Advantage ^a	COMSOL multi-physics; simple to implement	Facchin et al. (2015)
	Disadvantage	Construct level set function is difficult	
Phase field	Capability	Compound droplet	Zhou et al. (2008)
	Advantage ^a	COMSOL, MOOSE; multi-physics environment	
	Disadvantage	Computationally challenging for other	
Smoothed particle Hydrodynamics	Capability	Particle-based (RBC)	Wang et al. (2008)
	Advantage ^a	Abaqus; large deformation; excellent conservation	Wu et al. (2015)
	Disadvantage	Setting boundary conditions is difficult, weak at multiscale modeling	
Finite-element method ^a	Capability	Amoeboid cells, compound capsule, Maxwell solid material	Drury and Dembo (1999) Luo et al. (2014)
	Advantage ^a	Abaqus, ADINA	
Lattice Boltzmann method	Capability	Droplet, capsules, RBC and vesicles	Gupta et al. (2014)
	Advantage	Maintain sharp interfaces	Kusters et al. (2014)
	Disadvantage	Lack of strict mass conservation, macroscopic properties cannot be prescribed as input parameters	
Front tracking	Capability	Non-spherical/compound capsule	Tasoglu et al. (2010)
	Advantage	Robust solution, sharp interface method	Hassanzadeh et al. (2017), Luo and Bai (2017)
	Disadvantage	Complexity	
Boundary element method	Capability	Droplet, compound droplet	Haider and Guilak (2002)
	Advantage	Efficient: only the boundary of the domain needs to be discretized	Zinchenko and Davis (2006)
	Disadvantage	Cannot solve entering a sharp edge corner problem	
Immersed boundary method	Function	Coupling between fluid and solid	Kan et al. (1998)
	Capability	Compound droplet model with elasticity and viscosity	Marella and Udaykumar (2004) Leong et al. (2011)
	Advantage	Simple mesh: move objects or deform without remeshing	
Immersed fluid–solid interaction	Capability	Compound capsule with nucleus	Casquero et al. (2017)
	Advantage	Eulerian mesh for fluid, Lagrangian mesh for particle	
	Disadvantage	Computationally expensive	
Dissipative particle dynamics	Capability	Complex cell structure, membrane and skeleton	Peng et al. (2013) Yazdani and Karniadakis (2016)
	Advantage	Multiscale simulation; sub cell scale	
	Disadvantage	Computationally expensive	

^aEasy to implement: commercial software/package is available

excellent in Newtonian and low viscosity ratio fluid system. It can also simulate non-Newtonian or viscoelastic fluid through user-defined functions. Methods at the bottom rows

of Table 1 are usually computational resource consuming and less accessible for most researchers and engineers (Peng et al. 2013).

Numerical algorithms have been used in the simulation of particle squeezing through a narrow confinement are presented in Table 1. Among codes reviewed in Table 1, ANSYS Fluent is a powerful commercial package for multiphase flow modeling. It has been used to simulate Newtonian and power-law droplets under confinement. It can potentially be implemented to simulate a viscoelastic droplet squeezing problem. Abaqus and Adina provide a platform to simulate solid particle-squeezing problem with constitutive equations such as the neo-Hookean (Luo et al. 2014; Zhao et al. 2015) or Maxwell model (Shirai et al. 2003).

The same physical model can be simulated by different numerical methods. For example, a compound droplet squeezing through a narrow confinement has been conducted by the Volume of Fluid method (Zhang et al. 2015), immersed boundary method (Hua et al. 2014; Kan et al. 1998), boundary element method (Toose et al. 1999), phase-field method (Zhou et al. 2008), front-tracking method (Luo and Bai 2018; Muradoglu and Gokaltun 2005; Tasoglu et al. 2010), and Smooth Particle Hydrodynamicist (SPH method) (Wang et al. 2008). Advantages and disadvantages are discussed in Table 1.

Besides above commercial codes, a fluid static analysis tool, surface evolver (Berthier and Brakke 2012), is a quick, simple, and open-source package. The first public version of surface evolver was released in 1989. Surface evolver calculates the surface curvature by minimizing the total energy of liquid interfaces. However, the code is not capable to solve complex fluid/solid constitutive equations. Table 2 presents the commercially available and open-sourced software with their applications and specific features relevant to the study of particle squeezing through a narrow confinement.

Some in-house codes were developed to solve non-standard boundary conditions or complex constitutive problems. For example, the fluid–solid interaction (FSI) modified version of HARVEY (Gounley et al. 2017) (an LBM-based code) can handle compound capsules flowing through a confinement. However, many codes are neither open-source

nor commercialized, and further usage and development of these codes are mostly discontinued.

2.3 Operation parameters

2.3.1 Transit time

The transit time of a particle squeezed through a constricted confinement is mediated by the physical properties of particles and carrier fluid as well as their interactions with the confinement walls [collision and friction (Byun et al. 2013)]. The transit time can be used to evaluate the properties of the dispersed phase such as stiffness and viscosity (Tsai et al. 2014). In low capillary number pressure-driven flow, the transit time can be characterized by pressure signals (Zhang et al. 2017). In an electric field, the transit time can be estimated by the phase difference and the amplitude ratio of electric signals (Zheng et al. 2012). Further analysis of transit time can be used to estimate cell properties and cell types (Chen et al. 2011). For example, due to viscosity difference of cells, the motion profile or the $L-t$ relation (advancing length and time relation) is different for different types of cells. The $L-t$ relation tends to be linear at a constant pressure aspiration pipette (Hochmuth 2000), but non-linear at constant flow operation (Tsai et al. 2014).

A summary of transit time for a droplet, cell, and solid particle is given in Table 3. By definition, the transit time is the duration that it takes to transport a particle from the entrance to the exit of a narrow confinement. According to the continuity equation, a larger dispersed phase needs more flow time (Bow et al. 2011). Besides, the transit time is a function of operation conditions, structures, and physical properties.

In the case of a Newtonian droplet in the non-co-flow regime (carrier fluid is not coflowing with the dispersed phase inside the confinement), the transit time is inversely proportional to the product of average velocity and the confinement cross-sectional area. For some cases, the transit time can be corrected to a coefficient or changed into

Table 2 Available numerical solvers (commercial or open-sourced) used in previous research

Solver	Applications	Remarks	References
ANSYS fluent	Droplet/cell	Best convergence for viscosity ratio < 1000	Darvishzadeh and Priezjev (2012) Zhang et al. (2014) Zhang et al. (2018)
Abaqus	Solid particle	Visco-hyper-elastic solid neo-Hookean model	Luo et al. (2014) Zhao et al. (2015)
ADINA	Solid particle	Maxwell solid material	Shirai et al. (2003)
Surface evolver	Droplet/particle	Minimal surface energy by a gradient descent method	Brakke (1992)

Table 3 Available analytical/empirical transit time of particle squeezed through a narrow confinement

Type	Transit time (τ)	Comments	References
Droplet	$(V_D + V_C)/\bar{U}A_C$	Estimation from mass conservation assuming no co-flow; V_D and V_C are the volumes of droplet and channel, respectively; $\bar{U}A_C$ is the product of carrier fluid averaged velocity (\bar{U}) and confinement cross-sectional area (A_C)	Zhang et al. (2017)
	$\propto (Ca - Ca_c)^{-1/3}$	Flow-induced droplet squeezing through lattice of spheres. Ca is the capillary number, and Ca_c is the capillary number below which trapping occurs	Zinchenko and Davis (2008)
	$\propto (Bo - Bo_c)^{-1/2}$	Gravity-induced squeezing time. Bo is Bond number, and Bo_c is a critical bond number for trapping	Ratcliffe et al. (2010)
	$1.37 \frac{\mu V_0^{2/3}}{\sigma R \epsilon^2 \cos \theta_d}$	Droplet wicking into a capillary bundle. Useful for paper-based microfluidics. σ is the surface tension coefficient and θ_d is dynamic contact angle	Middleman (1995)
Cell	L/\bar{U}	For a long channel, where L is channel's length and \bar{U} is the averaged velocity of the particle	Zeina et al. (2017)
	$\propto \mu^{1/7}$	Cell entry time increases with viscosity ratio (μ) according to a power-law	Zhou et al. (2007)
	$\propto R_c^{-0.615}$	A square channel with the arc-shaped confinement channel. R_c is the confinement's radius	(Shirai and Masuda 2013)
	$\propto R_c^{-0.5}$	An axisymmetric capillary channel of radius R_c	Shirai et al. (2002)
	$\exp\left(3.68 \frac{R_c}{R_p} - 4.77\right)$	WBC entrance time of microvascular bed. R_c is the radius of the cell, and R_p is the radius of the confinement	Fenton et al. (1985)
	$t_e = \left(\frac{\epsilon E}{\Delta \bar{p}}\right)^{\frac{1}{\beta}}$	t_e is the cell entry time, ϵ is the maximum strain, β is the power-law exponent, $\beta=0$ indicates a purely elastic solid, $\beta=1$ indicates a purely viscous fluid, and $\Delta \bar{p}$ is the mean pressure	Lange et al. (2015)
Particle	$\mu \left[\frac{4(R_{\max} - R_{\min})}{R_{\max}^2 (\Delta P - \Delta P_c) \tan \Theta} - \frac{1}{G} \right]$	Transit time for a Maxwell solid particle through an arc-shaped confinement. R_{\max} is maximum cell radius in radial direction, and G is the shear modulus; θ is a geometric parameter; ΔP is the pipette pressure drop	Shirai et al. (2003)
	$\propto h^{-2/5}$	Active vesicle in inelastic regime passing through a blind confinement. h is the height of the confinement	Fai et al. (2017)

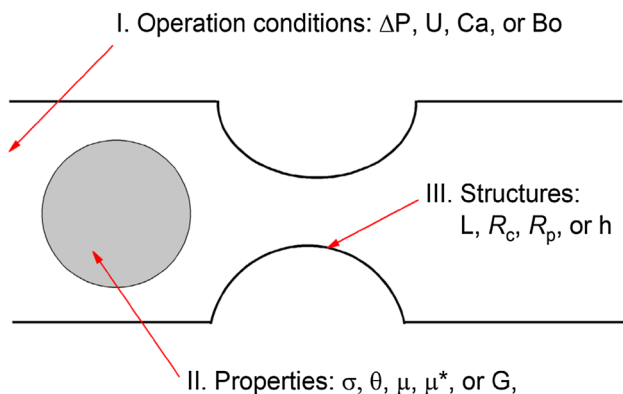


Fig. 2 Parameters influencing the transit time includes, I: operation conditions, II: properties, and III: structures. Symbols can refer to comments in Table 3

a power-law formula according to the transit velocity or characteristic dimension. Finally, the transit time may also change with the particle/cell's mechanical properties (Shirai et al. 2003; Tan et al. 2018a, b) such as Young's modules, shear module, surface tension, membrane compressibility modulus, and viscosity.

In Fig. 2, we summarized the key parameters influencing the squeezing time in Table 3. Symbols in Fig. 2 can refer to comments in Table 3. As summarized, the squeezing time was influenced by the operation conditions, particle properties, and the structures of the system. Besides the above-mentioned relations, numerical modeling of the transient time under the influence of squeezing pressure and pore size for a capsule have been conducted in Tan et al. (2018). Entrance time as a function of the viscosity ratio and capillary number for a viscoelastic droplet can be seen in Zhou et al. (2007).

2.3.2 Pressure

Pressure is a quantitative input to control the dispersed phase flowing with the carrier fluid (Pivkin et al. 2016). The critical pressure (the maximum extra pressure during squeezing) of squeezing a droplet through a narrow confinement is described by the Young–Laplace equation. The Young–Laplace equation is the most widely used design criteria in the microfluidics. However, there are several limitations in applying Laplace–Young equation: (1) Young–Laplace equation is only valid in a quasi-static situation, and non-static condition will induce sharper curvature or co-flow (Zhang et al. 2015); (2) viscosity influence has

not been taken into consideration, and extra pressure term exists in the design of non-Newtonian (Zhang et al. 2018) or viscoelastic droplet operation (Guevorkian et al. 2010); (3) for the existence of non-uniform stress or membrane stiffness; and (4) for channel with sharp corner, wetting behavior should also be considered (Zhang et al. 2014). Through the concept of equivalent surface tension, the Young–Laplace equation can also be used to characterize a solid particle.

A sudden pressure increase is observed experimentally for solid particles jammed in a confinement (Sendekie et al. 2016). At a low Reynolds number, the passing event can be linearly decomposed into a combination of two sub-models: (1) surface tracking of the immiscible dispersed phase and (2) the carrier fluid flow under a contraction-and-expansion confinement. A second-order relation between the squeezing pressure and operation velocity is reported.

Several groups are focusing on the analysis of the squeezing pressure of particles through confinement. Zhang et al. focused on the analytical analysis of a droplet squeezed through confinement under different cross sections (Zhang et al. 2014). Optimization of a mathematical relation for critical pressure, critical velocity, and minimal impulse has been analytically derived and numerically validated (Zhang et al. 2015). Benet et al. focused on semi-analytical pressure analysis of vesicle squeezing through a confinement channel or porous media (Benet et al. 2017; Benet and Vernerey 2016). Some recent studies on the non-Newtonian droplet generation resulted in pure numerical results under non-Newtonian constitutive equations. A summary of the driving forces considered in various studies is given in Table 4. At the same time, the resisting forces exist in the form of surface tension/viscosity/elasticity/shear modulus/adhesion of the particles.

Figure 3 presents pressure profiles from some key results of droplet/cell/particle squeezing through a narrow confinement. As seen in Category (I)-(a), according to the pressure profile, the squeezing event of a droplet through a confinement can be broken down into seven stages (Zhang et al.

2014): (a) initial state; (b) maximum pressure begins; (c) maximum pressure ends; (d) pressure balanced and is equal to the background pressure; (e) minimum pressure begins; (f) minimum pressure ends; and (g) rear part bouncing. However, for a solid particle with complex constitutive equations, there is no clear clue of stages (Park and Dimitrakopoulos 2013).

In Fig. 3j, in the quasi-static case, the circular channel provides the highest pressure. The six-edged constricted channel provides higher pressure than the rectangular channel. The critical pressure does not change too much with the variance of elongation ratio (Berthier and Brakke 2012). However, in the dynamic case, the pressure prediction is different.

Due to the existence of the phase interface, the pressure drop along the constricted channel is no longer linear. The pressure drop along the constricted channel is accumulative of (1) the major pressure loss determined by the Hagen–Poiseuille law, which linearly increases with the operation velocity, (2) the minor pressure loss due to the existence of contraction-and-expansion, which exhibits quadratic growth as a function of operation velocity in the constriction, and (3) the surface tension term, which changes dynamically with the droplet proceeding.

For five types of cross sections, the major pressure loss terms of the channels can be estimated analytically as summarized in the second column in Table 5. For an arbitrary cross section, the analytical form of major loss can be seen in (Van Hirtum et al. 2017). In quasi-static operation conditions, the critical pressure induced by the surface tension term can be estimated analytically in the third column in Table 5. Experimentally, the critical pressure can be obtained by the greatest difference between the transient squeezing pressure and the background pressure (a constant including Hagen–Poiseuille law term and the contraction-and-expansion term).

For a narrow confinement with angular cross sections, the wetting phase may occupy corners, while the

Table 4 Driving forces

Driving force	Remarks	References
Negative pressure at outlet	Aspiration pipette, aspiration-based bio-printing	Ayan et al. (2017)
Forward pressure at inlet	Deformability lost diagnose	Ito et al. (2017)
Constant flow rate	Filtration, sensing, cell labeling	Luo et al. (2015)
Gravity	Geoscience, enhanced oil recovery	Clark et al. (2005)
Electric	Electric charge caused by the triboelectric effect	Choi et al. (2013)
Acoustic vibration	Enhanced oil recovery, cell characterization	Beresnev and Deng (2010) and Beresnev et al. (2005)
Capillary action	Capillary action for super-hydrophilic wearable devices	Shou and Fan (2018)
Optic radiation	Cell property characterization	Vazquez et al. (2015)

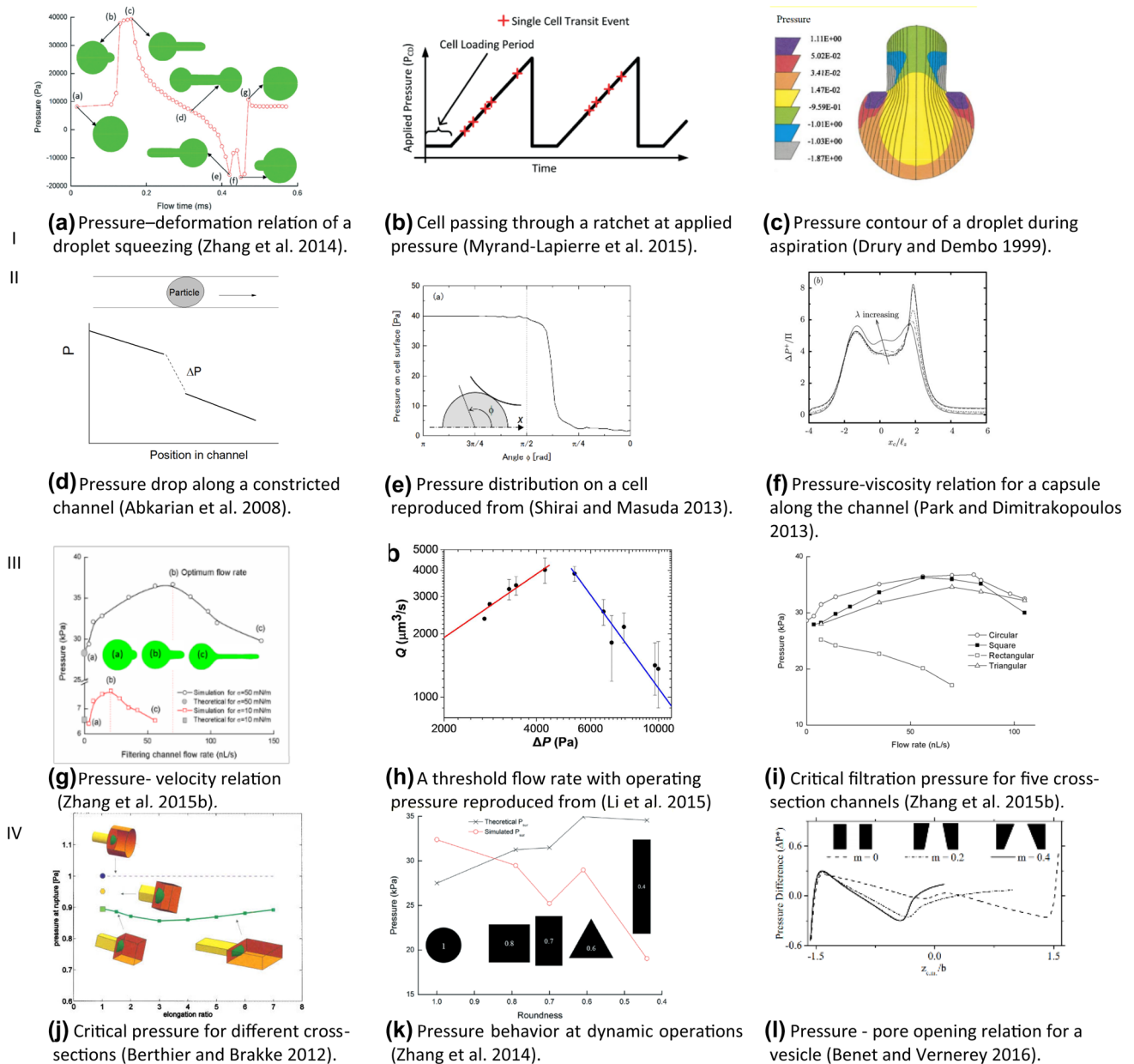
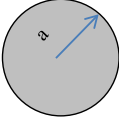

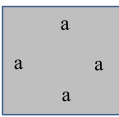
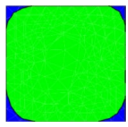
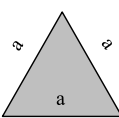
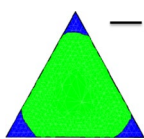
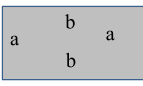



Fig. 3 Pressure of squeezing a particle through a narrow confinement. (I) relation with flow time, (II) relation with location, (III) relation with flow velocity, and (IV) relation with channel geometry. Copyright acknowledgment: (a) reproduced from (Zhang et al. 2014). (b) reproduced from (Myrand-Lapierre et al. 2015) with permission of The Royal Society of Chemistry. (c) reprinted from (Drury and Dembo 1999), Copyright 1999, with permission from Elsevier. (d) adjusted with permission from (Abkarian et al. 2008). Reproduced

with permission. ©IOP Publishing. All rights reserved. (f) reproduced from (Park and Dimitrakopoulos 2013) with permission from The Royal Society of Chemistry. (g) and (i) reprinted from (Zhang et al. 2015b). (j) reproduced from (Berthier and Brakke 2012) with permission. Copyright Wiley-VCH Verlag GmbH & Co. KGaA. (k) reproduced from (Zhang et al. 2014). (l) reprinted with permission from (Benet and Vernerey 2016). Copyright 2016 by the American Physical Society

Table 5 Designed geometries and their hydraulic resistances (2nd column), critical Young–Laplace critical pressures (2rd column), and numerical contours for a Newtonian droplet (last column) in the quasi-static flow. Table adapted from (Zhang et al. 2014)

Cross-sectional shapes of the filtering channel	Hydraulic resistances R_{hyd}	Critical Young–Laplace pressure P_{sur}	Droplet contour at inlet
Circular 	$\frac{8}{\pi} \eta L \frac{1}{a^3}$	$2\sigma \cos(\theta)/a - \frac{2\sigma}{R_{\text{cell}}}$	
Square 	$28.4 \eta L \frac{1}{a^3}$	$4\sigma \cos(\theta) \left(\frac{1}{a}\right) - \frac{2\sigma}{R_{\text{cell}}}$	
Triangular 	$\frac{320}{\sqrt{3}} \eta L \frac{1}{a^3}$	$12\sigma \cos(\theta)/\sqrt{3}a - \frac{2\sigma}{R_{\text{cell}}}$	
Rectangle 	$\frac{12}{1-0.63(a/b)} \eta L \frac{1}{a^3 b}$	$2\sigma \cos(\theta) \left(\frac{1}{a} + \frac{1}{b}\right) - \frac{2\sigma}{R_{\text{cell}}}$	

In the last column, the green contour is the droplet; the blue contour is the carrier fluid. The scale bar is 1 μm

non-wetting phase occupies the confinement center (Blunt 2001). A circular confinement allows only one phase occupying the cross section at low velocity. After co-flow, the droplet and carrier fluid flow together through the confinement. However, the critical pressure will change for a non-wetting droplet as shown in the corresponding simulation result in the last column of Table 5. With the increase of the operation velocity, the carrier fluid compresses the droplet and thus influences the critical pressure.

Besides the squeezing pressure mentioned above, researchers in biology care the critical pressure of capsule breakup, which was found follows the Weibull distribution (Le Goff et al. 2017).

2.3.3 Velocity

Velocity is a key operating parameter. For example, the migration velocity in a narrow-constricted channel is a measure of cancer cell invasiveness (Lautscham et al. 2015). The velocity is mainly determined by cells' adhesion, nuclear volume, and stiffness. When different particles (such as solid particles with different stiffness or a mixture of healthy cells/unhealthy cells with less deformability) enter a narrow confinement, the pressure–flow time relationship and the velocity field before channel entrance are different. By recognizing the difference, particle or cell detection/capture/sorting/counting can be conducted (Ren et al. 2017; Guo and Ma 2011).

Velocity and operation pressure are coupled parameters. When the operation velocity increases, an optimized condition, which provides the highest filtration pressure, can

be observed (Zhang et al. 2015). On the opposite, with the increase of operation pressure, a threshold velocity (flow rate) was also found (Li et al. 2015).

Through the optimization of operation velocity, two critical velocities were proposed for a droplet squeezing process. (1) The first one is the co-flow critical velocity. The co-flow critical velocity happens at the droplet entry stage. It can be used to predict the co-flow (Zhang et al. 2015) of the droplet and the carrier fluid, above which the carrier fluid and the droplet flow together into the constricted channel. Below the co-flow critical velocity, the flow at the channel inlet can be considered as a single-phase flow. However, after co-flow, the behaviors of droplet become less predictable (or mostly empirical description), and the thin lubrication film assumption becomes invalid. (2) Another critical velocity (Zhang et al. 2017), the minimum impulse critical velocity with a minimized momentum, was derived mathematically for a droplet with the viscosity ratio of 1. The minimum momentum is a balance of the second-order (with respect to the operation velocity) pressure loss and the inversed transit time relation under the constraint of finite droplet volume.

2.3.4 Non-dimensional parameters

To describe the flow status, non-dimensional ratios such as viscosity ratio, confinement ratio, and deformation index are commonly used. Reference (Chung et al. 2008) non-dimensionalized the Navier–Stokes equation in the simulation of a viscoelastic droplet squeezing. Reference (Barakat

Table 6 List of non-dimensional parameters

Non- dimensional parameters	Function
<i>Re</i> $Re = \rho Vd/\mu$ $Re=0$ Creeping	Flow regime of the carrier flow and transportation process optimization. d is the characterized dimension of the channel
Ca $Ca = \mu U/\sigma$ Droplet. $Ca = \infty$, jetting $Ca = \mu U/E_h$ Elastic particle $Ca = \mu U/G_s$ Elastic capsule	Capillary number: a multiphase flow parameter deciding co-flow behavior (Zhang et al. 2017a, b), flow regime (Thanh Hoang et al. 2017), and passing/stuck (Luo and Bai 2017)
Bo $Bo = \Delta\rho gR^2/\sigma$ $Bo < 10^{-5}$, gravity is negligible	Bond number: a multiphase flow parameter describing the shape of droplet and: trapping/squeezing flow regime under gravity (Ratcliffe et al. 2012). Droplet breakup under buoyancy (Olgac et al. 2006)
We $We = \rho u^2 L/\sigma$ Most microfluidics, $We < 1$	Weber number: a multiphase flow parameter describing deformation of droplet
Wi $Wi = \lambda U/L$ $Wi = 0$, Newtonian fluid	Weissenberg number: a rheology parameter describing fluid elasticity, viscoelastic property (Izbassarov and Muradoglu 2016)

and Shaqfeh 2018) non-dimensionalized governing equations for a vesicle squeezing modeling. Five most commonly used non-dimensional parameters are summarized in Table 6.

Reynold number (Re) is the ratio of the inertial term compared to the viscous term of the carrier fluid. It is independent of the property of the dispersed phases. Navier–Stokes equations can be linearized at a low Reynold number (Stokes flow with $Re \ll 1$).

Capillary number (Ca) is the ratio of shear stress and surface tension. It can be expressed as: $Ca = \mu U/\sigma$ for a droplet, μ and U are the viscosity and velocity of the carrier fluid, $Ca = \mu U/E$ for a solid particle with E_h as the membrane bending stiffness (Arata and Alexeev 2009), and $Ca = \mu U/G_s$, with G_s is the membrane's shear modulus of a capsule (Park and Dimitrakopoulos 2013) or $Ca = \mu U_{\max}/E$ using the maximum velocity (Luo and Bai 2017). A large or infinite Ca number corresponds to jetting (Tsai and Miksis 1994) with negligible stiffness. In a chip design, Ca influences the co-flow behavior (Zhang et al. 2017a, b), flow regime (Thanh Hoang et al. 2017), and passing/stuck behavior (Luo and Bai 2017). An increased Ca number was reported to decrease the viability of cells during filtration (Zhao et al. 2017) due to high shear rate. Ca number is the most widely used non-dimensional parameter in the particle-squeezing problem.

Bond number (Bo) is the ratio of the buoyancy and interfacial term. Bo number can be expressed as, $Bo = \Delta\rho gR^2/\sigma$ for a droplet. Here, $\Delta\rho$ is the density difference between two fluids, R is the radius of the droplet, and σ is the surface tension coefficient. The surface tension or stiffness plays a role in maintaining the original shape of the particle and resisting deformation caused by the shear stress, gravity (Ratcliffe et al. 2012), and buoyance (Olgac et al. 2006).

Weber number (We) is the ratio of the inertia and surface tension. It is a multiphase flow parameter useful in analyzing droplets formation and thin-film flows. We number was reported to decide the co-flow critical velocity for a droplet entering constricted channels (Zhang et al. 2015). For cells and particles, We number has not been reported yet to be useful.

Weissenberg number (Wi) is the ratio of elastic and viscous forces. It is a rheology parameter quantifying viscoelastic effects. For complex fluids, Wi number is defined as, $Wi = \lambda U/L$. Here, λ is the characterized relaxation time, L is the characteristic length, and U is the characteristic velocity (Izbassarov and Muradoglu 2016). Similar to the Wi number, the Deborah number ($De = \tau_c/\tau_p$, τ_c stands for the “relaxation time” and τ_p for the “time of observation”) can also be used to quantify viscoelastic effects (Luo and Bai 2018).

3 Summary of applications

The physical model of a particle squeezing through a narrow confinement has been widely used in various applications for a long time. A summary of historical view for the applications of the model is summarized in Table 7. The model was first used in chemical engineering for droplet emulsion and enhanced oil recovery. Gradually, bio-engineers started to use confinement to measure and manipulate cells or tissues. After years of development, many numerical techniques and mathematical models have been developed towards the design and optimization of lab-on-a-chip devices. Recently, the model has been used in pathology (CTC metastasis, etc.) and biotechnology such as the drug delivery [ion (Danielczok et al. 2017) or macromolecular (Sharei et al. 2013)] and cell therapy.

Table 7 History of applications of the particle squeezing through a narrow confinement

Years	Popular applications
1980s and before	Emulsion
1990s	Enhanced oil recovery
	Cell- property measurement
	Compound droplet simulation
2000s	Viscoelastic droplet
	Encapsulation
	Droplet generation
2010s	CTC metastasis
	Drug delivery
	Multiscale modeling

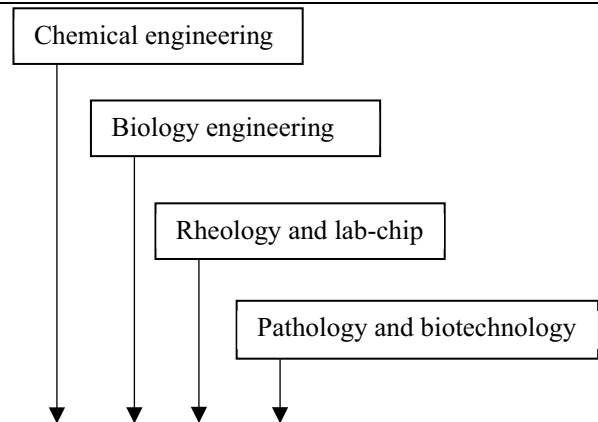


Table 8 shows a more detailed summary of the fields and applications of particle squeezing through a narrow confinement.

3.1 Pathology and healthcare

Cell migration through a confined space is a fundamental problem that underlies diverse pathological processes. Constricted channels in the human body are mostly in the form of capillary obstructions. Capillaries can be blocked by a bigger cell or a blood clot. In disease detection or some in vitro techniques, cell's deformability is the main focus of research.

In pathology, the cell deformability loss is a common symptom of many diseases. Since 1972, it has been known that a decreased shear modulus can cause a difficult recovery (Shelby et al. 2003) from Malaria-infected, sepsis infected, and oxidative red blood cell (RBC). Infected RBCs cannot enter the openings (about 2 μm) in the spleen. Bigger white blood cells (WBCs) can get stuck in a pulmonary capillary (Shirai et al. 2003). A larger blood clot can block a vessel in the brain or heart, which causes hypertension, ischemic cerebral aneurysms, stroke, or heart attack. In legs, a disease called deep vein thrombosis (DVT) is caused by a blood clot or embolus blocking (Anselmo and Mitragotri 2016).

A type of rare cell in the blood is the circulating tumor cell (CTC). Due to partial loss of actin filament or disorganization of microtubules, a tumor cell becomes stiffer than healthy cells. CTCs are the main reason for cancer metastasis. It is also found to be a potential indicator of early tumor formation. Due to the presence of CTCs or CTC clusters (Aceto et al. 2014) in the peripheral blood, cancer in patients can be detected before the onset of clinical symptoms (Alix-Panabières and Pantel 2014; Fabbri et al. 2013; Hong and

Zu 2013; Kim et al. 2009). Given the high incidence of cancer and the lack of successful treatments for most types of cancers, pathology of cancer metastasis and cell migration continues to be significant research topics.

3.2 Microfluidics and drug delivery

Deformability-based detection/isolation separates droplets/cells/particles by their different mechanical properties. Devices performing cells' separability are cell cytometers, size-based cell sorters, or deformability filters (Bow et al. 2011) and membranes (Sun et al. 2018). The deformability loss of a cell is both a cause of and a biomarker for disease states. The individual cell's mechanical properties can be used as biomarkers for many diseases including cancer, malaria, asthma, and arthritis. Rare cells like reproductive (Luo et al. 2015), or circulating tumor cells (Vazquez et al. 2015) are designed towards separation from plasma or abundance of cells like red blood cells. To detect the deformability lost, many physical-principle-based techniques can be seen in Lee et al. (2015). The rare cell separation technologies are summarized in Chen et al. (2014).

In drug delivery, particle squeezing exists in two aspects: (1) open crack on and permeation through the cell membrane in intracellular delivery of macromolecules, such as drugs, carbon nanotubes, proteins, and siRNA, is a challenge both in research and clinic applications. Cell squeezing using (around half to one-third of the cell's diameter) microfluidic constricted channels can help significantly in the drug delivery (Sharei et al. 2013). A company named "SQZ" is working on the method of drug delivery of this method. (2) Material property test: biomaterial mechanical properties such as the deformability are an important parameter for the polymeric microparticles. The ability to dynamically

Table 8 Applications of particles' squeezing through a narrow confinement

Field	Applications	Function and comments	References
Pathology and healthcare	Blood clotting	Platelet under confinement	Shen et al. (2009) and Yazdani and Karniadakis (2016)
	Brain stroke	Stroke recovery and blockage removal	Zhang and Drapaca (2016)
	RBC filtration	RBCs pass through the interendothelial slits in the spleen	Peng et al. (2013)
	CTC metastasis	Tumor dissemination in distant organs	Au et al. (2016)
	Pulmonary embolism	Leukocyte and particle blockage in pulmonary microvascular	Shirai and Masuda (2013), Watson et al. (2012)
	Deep vein thrombosis	A clot blocks the circulation in vein of lower legs, thighs, or arm	Chiu and Chien (2011)
	Drug delivery	In vitro and ex vivo intracellular delivery	Stewart et al. (2016)
	Assisted reproductive technologies	To study of oocyte structure and function	Luo et al. (2015)
Microfluidics	Droplet generation	Generate droplet through a constricted channel	Zhou et al. (2006)
	Flow cytometry	Cell counter for infected red blood cell	Bow et al. (2011)
	Micropetite	Cell and tissue property measurement	Hochmuth (2000)
	Bio-printing	Tissue pick- and- place	Datta et al. (2017)
	Cell labeling	Mark cell with proteins	Kollmannsperger et al. (2016)
	Cell reorganization	Cell transit time is an indicator of mechanical property	Chen et al. (2011)
	Microfiltration	Cell filtration and protein removal	Beckman and Barbano (2013)
Chemical engr	Emulsification	Break-up droplet into smaller ones	Rosenfeld et al. (2014)
	Enhanced oil recovery	Increase the movability of oil in porous media	Beresnev and Deng (2010)
	Packed bed	Improve contact between two phases	Zinchenko and Davis (2017)
	Printer dynamics	3D printing and bio-printing	Tan (2016)
	Clogging dynamics	Bacteria blocks particle transport	Sendekie et al. (2016)
	Capillary valve	Pressure controlled fluid regulation	Berthier and Brakke (2012)
	Others	Microlens (Optical)	Light manipulation
Droplet transducer (Electronical)		Countering capillarity with electrokinetics	Vogel et al. (2005)
Nano-pipette (material)		Carbon nanotubes filled with metals	Schebarchov and Hendy (2011)
Hotspot cooling (Thermal)		Electric driven droplet cooling	Bindiganavale et al. (2012)
Wearable devices (Thermal)		Wearable device sweat removal	Shou and Fan (2018)

pass through various obstructions and recovery their shape is the main concern in this test. The microconstricted channel has become a standard and powerful tool for capsule property test. For example, to characterize the robustness of fluid-filled capsule, the critical passing pressure and a breakup pressure should be taken into consideration. The confinement ratio for soft microgel (Hendrickson and Lyon 2010) tests can reach, $D/d=1/10$ or even lower for the cell membrane test (Mulligan and Rothstein 2011).

3.3 Chemical engineering and other fields

Particle clogging (Massenburg et al. 2016) or blockage occurs at a significant particle stiffness (Wu and Feng 2013).

Laser surface processing (Xu et al. 2017) and bacteria (Sendekie et al. 2016) can reduce or delay the clogging of particles in a channel. Clogging problem in microfluidics has been reviewed in a recent review (Dressaire and Sauret 2017).

A capillary burst valve uses the liquid interface before the enlargement until the pressure exceeds the threshold value, $c\sigma/R$, where c is an efficiency parameter dependent on the cross-sectional geometry and contact angle (Berthier and Brakke 2012), σ is the surface tension of the droplet, and R is the radius of the constricted channel. After the maximum pressure, the fluid will suddenly burst into the enlargement. The capillary valve is the only kind of "passive" valve, which does not require other energy source, but only the interface itself.

A droplet penetrating through a porous media can be used to understand a wide range of industrial problems (Middleman 1995) such as ink penetration into the paper, enhanced oil recovery, and wastewater treatment. The permeability of a porous medium can be increased by mechanical shaking (Beresnev et al. 2011) or adding acoustic waves (Beresnev et al. 2005)/nanoparticle (Xu et al. 2015).

Thermal comfort plays a significant role in the best performance of apparel (daily clothing, sports clothing, or medical clothing) or wearable devices. Directional flow (Shou et al. 2014a, b, c) is usually preferred due to the requirement of sweat removal in fibrous material. Sweat is a super-hydrophilic droplet. The removal of sweat has been studied at the micro and nanoscale (Shou and Fan 2018) at fast absorption or removal rates (Shou et al. 2013) under gravity (Shou et al. 2014), in the complex (Shou et al. 2014) or optimized (Shou and Fan 2015) geometries.

The model of a droplet confined in a constricted channel has also been applied in other engineering areas. For instance, in optical engineering, a constricted channel is designed as a lens holder, while a droplet is designed as an optical lens. In thermal engineering, droplets (Bindiganavale et al. 2012) have been used in electronic components cooling: when a coolant droplet moves across the hotspot plate (a constricted channel), it picks up and removes heat (Park and Nam 2017). Figure 4 shows some of the applications mentioned above. Several multiphysics research studies will be reviewed in Sect. 6.3.

4 Narrow confinements

4.1 Functions

As seen in the applications mentioned earlier, the confinements play mainly two roles: measuring and manipulating.

4.1.1 Measuring

In biological studies, confinements are mostly in the form of pipettes (static method) and constricted channels (continuous flow). Pipettes are tools working in a quasi-static state, while constricted channels provide a higher velocity flow.

Researchers became interested in the quantitative measurement of cell properties, because cell properties are indicators of diseases. Mechanical properties of the cell membrane (Prévost et al. 2015), nucleus (Guilak et al. 2000), and cell aggregation (Khalifat et al. 2016) can be measured based on the relation between deformation and applied force using the micropipette aspiration. The most extensively used micropipette is the straight pipette. Mechanical behavior of cell and tissue aspiration through a straight pipette has been well-studied for Newtonian by the Young–Laplace equation

and viscoelastic droplets by the equation set in Reference (Guevorkian et al. 2010). A wide variety of properties have been measured such as the static (Zhang et al. 2014) and dynamic (Brosseau et al. 2014) surface tension coefficient of a droplet, the Young's modulus of a cell (Zhao et al. 2015) or tissue aggregate assembly (Aoki et al. 1997) for a solid model, the indentation elastic modulus (Argatov and Mishuris 2016), compressibility modulus (Evans et al. 1976) of cell membrane, adherent module for self-propelled vesicles (Lagny and Bassereau 2015), etc. A recent review of cell aspiration using a pipette can be found in (Hochmuth 2000). A review of tissues under aspiration using a pipette and competing for non-pipette techniques is given in (Khalifat et al. 2016). Other reviews can be found for the pipette applications in molecular mechanics (Lee and Liu 2014), for the measurement of properties of red blood cells (Kim et al. 2012), and for the micropipette aspiration (Hochmuth 2000).

A narrow-confinement-based measurement of cell mechanical properties is given in (Xue et al. 2015). A pipette was employed in the research of the active cellular response in cell aggregation pulsed contractions, cell aggregation, and cell. Narrow confinement can also be used for cell counting in CTCs. Confinement channels of various geometries have been developed such as colonial, tapered, or ratchet. These confinement channels were reported to have various advantages: (1) the ratchet was claimed to improve diagnostic sensitivity of diseased red blood cell (Guo et al. 2016); (2) a tapered confinement channel can provide higher shear stress; and (3) a colonial channel can increase the critical pressure (Aghaamoo et al. 2015). However, these non-straight pipettes were used mainly in the surface tension measurement, due to the lack of strict mathematical descriptions (Hochmuth 2000). Selection of pipettes or constricted channel should balance measuring speed and measuring precision (Wyss 2015). Commonly, the constricted channel is a quick and convenient approach, but its precision is not satisfying.

4.1.2 Manipulating

Manipulating includes dispensing, sorting, and positioning,

1. Positioning. Holding and placing are important functions of a confinement (mainly in the form of a pipette). The holding pipette provides controllable forces (like a tweezer) on a particle in various applications such as coalescence (Frostad et al. 2016), cell imaging (Yoshino et al. 2017), droplet storage (Boukellal et al. 2009), intracytoplasmic sperm injection, and pick-and-place bio-printing. The operation pressure should be lower than the Young–Laplace critical pressure for a Newtonian droplet. For solid particles and cells, a higher pres-

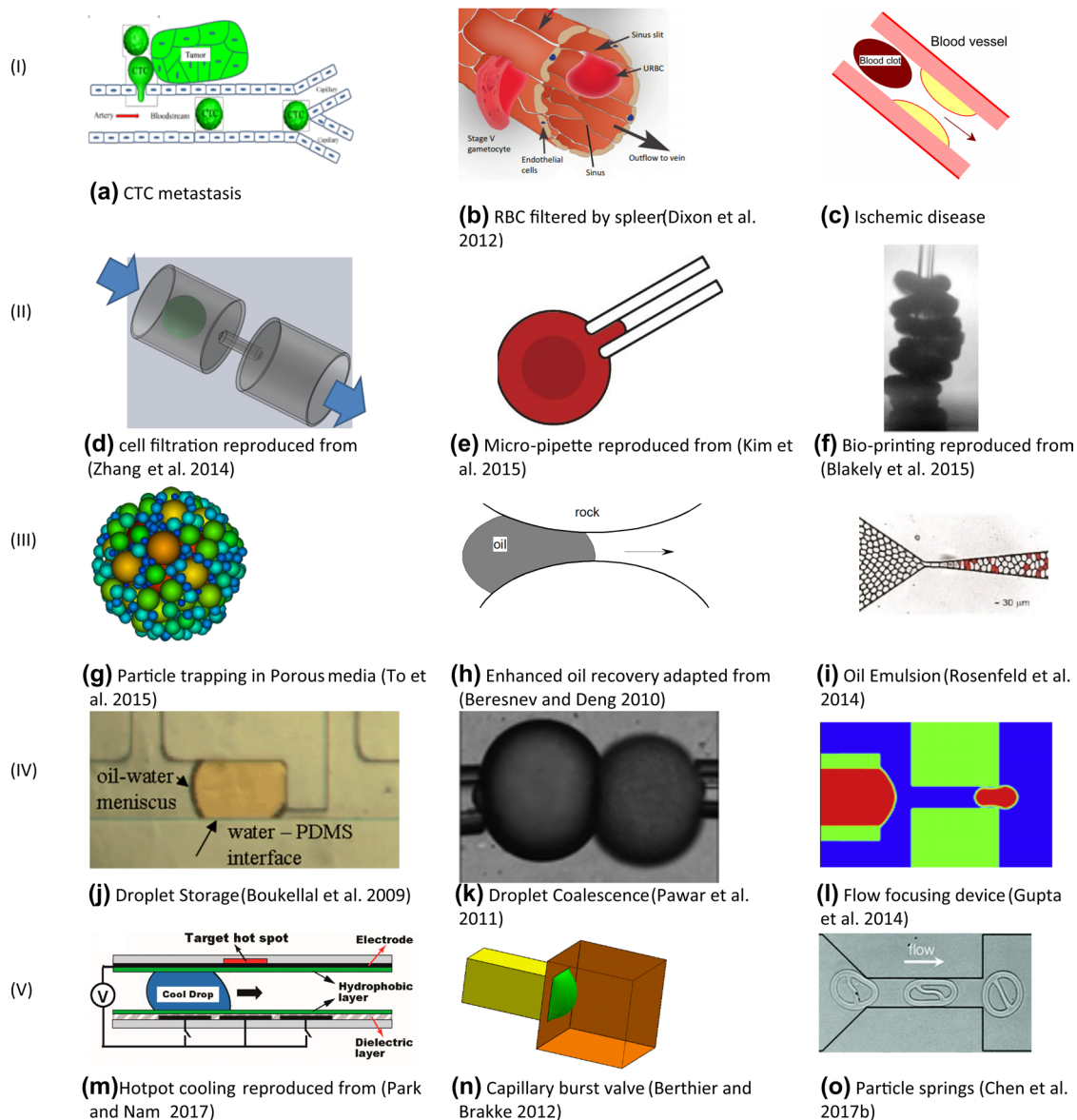


Fig. 4 Application of model. (I) **a–c** in pathology, (II) **d–f** in disease-related treatment, (III) **g–i** chemical engineering application, (IV) **j–l** droplet operation, and (V) **m–o** other engineering applications. Copyright acknowledgment: (b) reproduced from (Dixon et al. 2012). Copyright 2012, with permission from Elsevier. (g) reproduced from (To et al. 2015) with permission from ASCE. (i) reproduced from (Rosenfeld et al. 2014) with permission from The Royal Society of Chemistry. (j) reproduced from (Boukellal et al. 2009) with permission

from The Royal Society of Chemistry. (k) reproduced from (Pawar et al. 2011) with permission from The Royal Society of Chemistry. (l) reproduced from (Gupta et al. 2014). Copyright 1999, with permission from Elsevier. (n) reproduced from (Berthier and Brakke 2012) with permission. Copyright Wiley-VCH Verlag GmbH & Co. KGaA. (o) reproduced from (Chen et al. 2017b) with permission from The Royal Society of Chemistry

sure can be applied due to the elasticity of the dispersed phase. Competing techniques of holding pipette using multiphysics methods can be applied such as an acoustic tweezer and optic tweezers (Prévost et al. 2015).

2. Sorting. Examples include size and deformability-based cell filtration (Li et al. 2017) and the translocation of

a deformable particle across pores at the nanoscale (Pegoraro et al. 2014).

3. Dispensing. In cases like droplet generation, emulsion, or printing, a narrow-constricted channel provides shear stress (Genovese and Sprakel 2011). At high velocity

or high viscosity, the behavior of the dispersed phase becomes less predictable.

4.2 Arrangement

Confinement is one of the main interests of this review. The material of confinements is usually stiffer than the deformable particles. Glass, PDMS, or rock are commonly available materials for confinement. Besides, recent new trials have employed flexible confinement (Sohrabi et al. 2018) and non-solid confinement (Xie et al. 2016).

Different from a weak confinement, there is direct contact, and strong interaction exists between the dispersed phase and the narrow confinement. Confinement provides shear or normal stress to deform the particle. For example, the constricted channel in a flow-focusing device provides shear stress to cut off the droplet (Zhou et al. 2006). The constricted channel in a cell-labeling device (Kollmannsperger et al. 2016) deforms a cell and open small cracks on the cell membrane. The shear stress in a confinement can induce clotting in blood flow (Shen et al. 2009). Similarly, venous thromboembolism (collectively referred to as pulmonary embolism and DVT) is also caused by a narrow-constricted blood vessel (Table 9).

Confinement channels exist in many forms such as bottlenecks, stenosis (Mittal et al. 2003), capillary blood vessel, sieve (Lorenceanu and Quéré 2003), short orifices, pores in porous media, rock cracks, etc. (Ralf et al. 2012). A wide variety of geometries and arrangements have been designed.

Bundles of small capillaries in the form of a lattice of a sphere (Zinchenko and Davis 2008) or pillars exist in applications such as ink penetration dynamics. Some complex confinements are designed to simulate porous media, with the form of multiple successive pillars, [cylinder (Chung et al. 2010), diamond (Han et al. 2015), triangle (Sarioglu et al. 2015), or ellipse (Chen et al. 2017a, b; Fang et al. 2014)].

Squeezing pressure of five cross-sectional geometries (circular, triangle, square, and two rectangles) are compared for droplet-based filtration in (Zhang et al. 2014). The circular and slit cases were compared using the same method in Li et al. (2017) through area strain rate towards the optimization of the filtration process.

Usually, the external flow confinements can process fluid with higher processing rates. However, the control accuracy for external flow confinements is not satisfying. The types of confinements commonly used in the literature are summarized in Table 10 and Fig. 5.

Recently, directional confinements are increasingly investigated. A typical confinement with a uniform cross section can only provide symmetric flow condition in an inversed flow. Differently, directional confinements can provide “directional flow”. For example, a tapered constricted channel (gradually changing cross section) or ratchet can provide an asymmetric pressure signature at the inverse direction of flow than along the direction of taper (Guo et al. 2012). Consequently, directional confinement with asymmetric threshold pressures can be used to filter particles with different

Table 9 Available confinements

Confinement geometry	Design purpose	References
<i>Along channel direction</i>		
Straight	Micropipette, cell filtration, Mitosis study	Fischer-Friedrich et al. (2014)
Tapered/conical	Droplet breakup, property measurement	Gai et al. (2016) and Kong et al. (2014)
Parallel plate	An analytical solution is available for droplet squeezing	Barthès-Biesel (2012)
Sinusoidal/cosine	Oil trapping, emulsion, droplet breakup	Beresnev et al. (2009), Lee (2010) and Olbricht and Leal (1983)
<i>Corrugations</i>		
Arc-shaped	Buoyancy-driven droplet breakup	Olgac et al. (2006)
Double bend	WBC through the pulmonary capillary, cell sorter	Shirai et al. (2003) and Xu et al. (2017)
Saw-tooth-shaped	Provides deformation and rotation	Christafakis and Tsangaris (2008)
Hyperbolic channel	Directional transportation by periodic half-open capillary channels	Comanns et al. (2015), Brouzes et al. (2009)
Shark teeth	Capsule dynamics, encapsulate droplet	Dawson et al. (2015)
<i>Cross-section</i>		
Circular	Rapid cell deformation	Abkarian et al. (2008)
Rectangular/square	Sieve, orifice, filter	Lorenceanu and Quéré (2003)
Triangular	Capsule trapping, CTC capture	Luo and Bai (2017) and Ahmmed et al. (2018)
Slit	To simulate the pore between circular pillar in porous media	Blunt (2001)
Ridges	Slit between endothelial cells	Xiao et al. (2016)
Ring	Stiffness-based particle sorting	Arata and Alexeev (2009)
	Pore constriction, porous media; droplet under gravity influence	Ratcliffe et al. (2012)

Table 10 Deformation and confinement evaluation

Index	Explanation	References
<i>Deformation index</i>		
$\frac{L-B}{L+B}$	Taylor Deformation Index. L is the maximum length of the droplet; B is the minimum length of the droplet. $DI=0$ means no deformation	Luo et al. (2015)
$\frac{L}{r}$ or $\frac{L}{D}$	L is the maximum length of droplet, r is the un-deformed droplet radius, D is the un-deformed diameter	Wetzel and Tucker (2001)
$\frac{P}{2\sqrt{\pi A}}$	P and A are the imaged perimeter and area of droplet, respectively	Gai et al. (2016)
$C \frac{e_1 - e_0}{e_1}$	e_1 is the ellipticity of after deformation, e_0 is the ellipticity before deformation, C is a correction factor	Vazquez et al. (2015)
<i>Confinement index</i>		
$\frac{A_D}{A_H}$	A_D is the cross section of un-deformed droplet, A_H is the cross section of constricted channel	Guo et al. (2012)
$\frac{r}{r_H}$	r is un-deformed droplet radius, r_H is the hydraulic radius of the constricted channel, $r_H = \frac{W_c H}{W_c + H}$, W_c and H are the width and height of the constricted channel, respectively	Gai et al. (2016)
$\frac{D-d}{D}$	D is the diameter of a droplet; d is the diameter of the constricted channel	She et al. (2012)

physical properties. These directional confinements have been developed to measure properties of cells and compound droplets (Kong et al. 2014), the shear, and compressive moduli for core–micro shell particles. It has also been used in the emulsion encapsulation of double-layered structure. Besides, the directional flow channels have been reported to improve the diagnostic sensitivity of diseased red blood cell (Guo et al. 2016).

As seen from Category (II), successive confinements were employed when one unit was insufficient. Furthermore, various cross sections as seen from Category (III) have been designed for different purposes. Besides, special designed confinements can provide particular functions. For example, in the deformability-based particle separation, the diagonal solid ridges can provide distinct paths to particles (Arata and Alexeev 2009), but straight ridges do not have this effect.

5 Particles and fluids

In most research studies, the disperse phase is the main focus. The cell in a pipette aspiration, the oil droplet in the enhanced oil recovery process, and the particle in a membrane separation are all examples of disperse phases. Droplet and solid particles under confinements are widely investigated disperse phases, while capsule and vesicles have seldom been discussed.

5.1 Dispersed phase

From the perspective of fluid mechanics, a particle squeezing through a confinement is similar to the problem of a multiphase flow under confinement. For the dispersed phase, several constitutive equations have been studied such as a

Newtonian droplet, Non-Newtonian (Drury and Dembo 2001), capsule (Park and Dimitrakopoulos 2013), fluid-filled elastic shells (Arata and Alexeev 2009), etc.

A droplet is important in microfluidics, because drops are considered as microreactors or transport cargos (Xu and Attinger 2008). The droplet model has a big advantage in modeling large deformations of the dispersed phase. The simplest droplet model considers only the surface tension, which tends to keep the droplet a spherical shape, and neglects all other mechanical properties such as viscosity and elasticity.

Elasticity is the most important mechanical property of a solid particle. To squeeze a particle through a constricted channel, the deformation energy includes the bending and stretching. The balance between the interfacial energy and the pressure-driven flow will either cause particle clogging or passing. For example, a soft particle can pass through the constricted channel, while the solid particle will most likely get stuck. A conversion called “equivalent surface tension” can be used to compare the surface tension and Young’s modulus of a solid particle (Hochmuth 2000).

There are no specified constitutive equations for cells or tissues. A cell is usually modeled either as a uniform droplet (with surface tension) or a solid particle (with elasticity). Mechanical behavior of a cell has been described either as a fluid (Newtonian, power-law, and linear viscoelastic) or a solid particle (linear elastic and hyper-elastic). A viscoelastic model is considered to provide the best description of the mechanics of the cell membrane and biological tissues. The RBC membrane behaves as a resilient viscoelastic shell. The rheology of a viscoelastic cell tends to change after severe mechanical deformation due to cytoskeletal remodeling (Yap and Kamm 2005).

A viscoelastic particle widely exists in chemical and petroleum engineering. Generally speaking, the

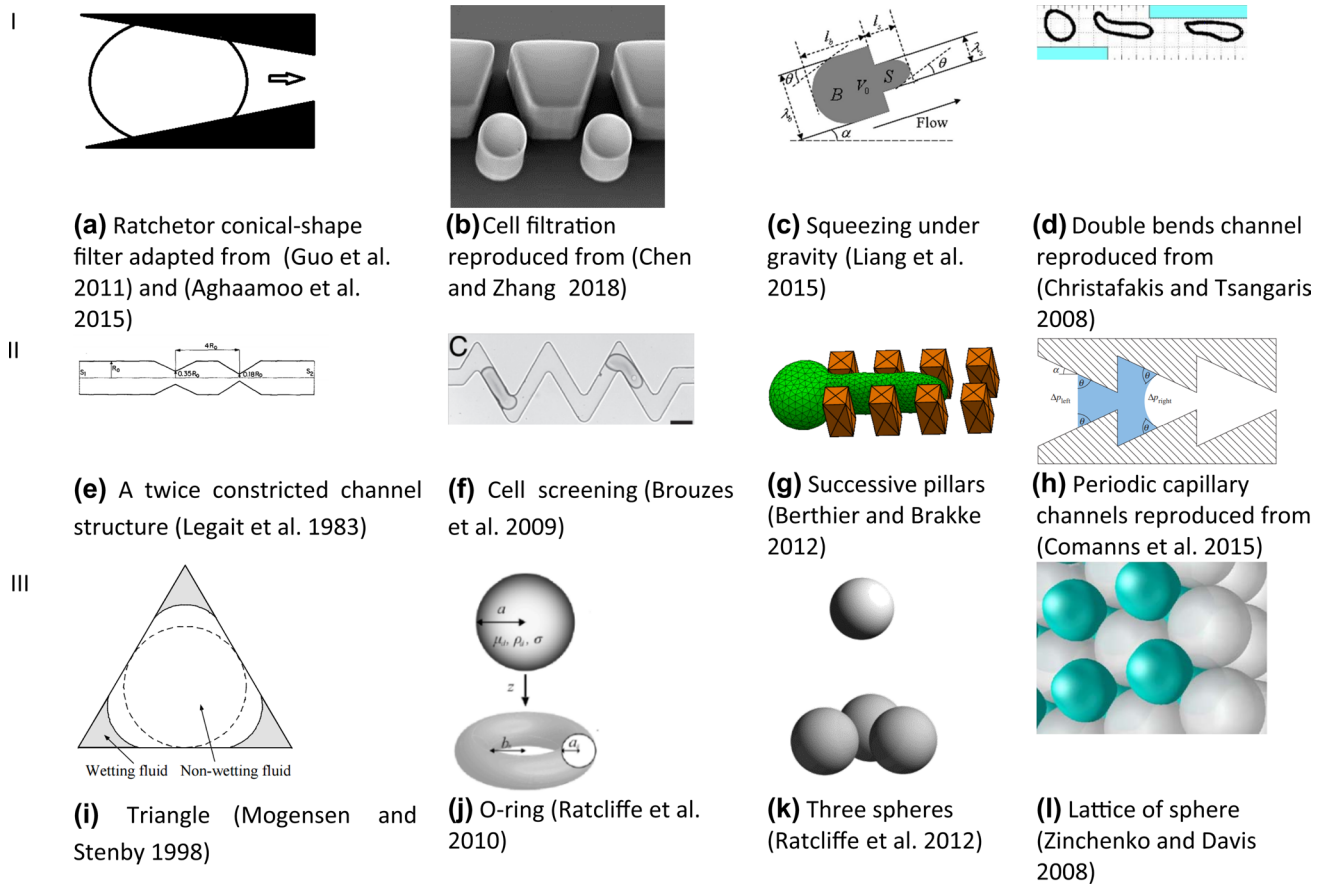


Fig. 5 Confinement channel geometry designs: (I) directional confinement, (II) periodic confinement, and (III) complex cross sections. Copyright acknowledgment: (c) reproduced from with permission of Springer. (e) reproduced from (Legait et al. 1983). Copyright 1983, with permission from Elsevier. (f) reproduced from (Brouzes et al. 2009) with permission. (g) reproduced from (Berthier and Brakke 2012) with permission. Copyright Wiley-VCH Verlag GmbH & Co.

KGaA. (i) reproduced from (Mogensen and Stenby 1998) with permission from Springer. (j) reproduced from (Ratcliffe et al. 2010). Reproduced with permission. ©IOP Publishing. All rights reserved. (k) reproduced from (Ratcliffe et al. 2012). Copyright 2012, with permission from Elsevier. (l) reproduced from (Zinchenko and Davis 2008). Reproduced with permission. ©IOP Publishing. All rights reserved

viscoelasticity inhibits the deformation of a droplet and decreases its mobility (Zolfaghari et al. 2017). Several viscoelastic constitutive models, including the Finitely Extensible Non-linear Elastic–Chilcott and Rallison (FENE-CR) model (Izbassarov and Muradoglu 2016) and Oldroyd-B constitutive model (Luo and Bai 2017), have been studied. The FENE-CR model is more realistic than the Oldroyd-B constitutive model, since it accounts for finite extensibility. A viscoelastic droplet under confinement has been simulated using the front-tracking method (Izbassarov and Muradoglu 2016) and volume of fluid method (Harvie et al. 2008). Under complex confinements, auxiliary meshes with a second-order accuracy can be used to track interfaces efficiently. However, the simulation of a viscoelastic droplet at a high flow rate, like an encapsulation of a droplet in a constricted channel, is not very accurate (Izbassarov and Muradoglu 2016).

Usually, a viscoelastic droplet generates extra stress at the wall of the constricted channel and induces complex deformations in the dispersed phase. Comparisons of the deformations of red blood cells (Tomaiuolo et al. 2009), healthy and sick red blood cells (Hassanzadeh et al. 2017), white blood cells, and circulating tumor cells (Zhang et al. 2014) have been conducted in theoretical and numerical studies.

From a structural point of view, capsules, vesicles, and hydrogels are complex particles. In capsules and vesicles, the membrane has a bending stiffness. A capsule has a highly stretchable structure with a thin elastic membrane enclosing a viscous fluid, while a vesicle has an inextensible membrane enclosing a viscous fluid (Barakat and Shaqfeh 2018). There are few studies of a vesicle under solid confinement due to technical difficulties in simulations (Barakat and Shaqfeh 2018). A hydrogel has a cross-linked latex structure which is swollen by a solvent (Li 2010). Other complex particles will further be discussed in Sect. 6.1.

5.2 Carrier fluid

The carrier fluid is the co-flow fluid (Zheng et al. 2012), lubrication film (Barakat and Shaqfeh 2018), or fluid at gutter (Zhang et al. 2014). The carrier fluid flows around the dispersed phase, transports shear stress, and deforms the dispersed phase. There is no significant difference in the wall shear stress (WSS) in a wide-open channel for different carrier fluids (Newtonian, power-law, and linear viscoelastic), but significant WSS difference has been reported in a highly constricted channel (Khambhampati 2013). For most applications, we reviewed in this topic, and there is less attention paid to the carrier fluid comparing to the dispersed phase.

At low operation velocities, the dispersed phase occupies most of the cross section. For a particle flow through non-circular cross sections with sharp corners, there are alternative flow paths at the gutter. The gutter was reported that the co-flow critical velocity has been analytically derived and numerically validated for a Newtonian droplet (Zhang et al. 2015). Results show good agreement between the mathematical formula and the numerical simulations for a stiff droplet, but not for compliant droplet with low-surface tension coefficient. The co-flow velocity has not been experimentally validated yet.

5.3 Deformation and confinement evaluation

The deformation of the dispersed phase depends on the flow conditions as reviewed in Sect. 2, constitutive equations of the droplet and the carrier fluid as reviewed in Sect. 5.1 and Sect. 5.2, and confinements as reviewed in Sect. 4. The shape of the droplet ranges from parachute-shaped to dumbbell-shaped during the process of squeezing through a constricted channel. Usually, the deformation is regular or ‘bullet-like’ for a Newtonian droplet and Newtonian carrier fluid (Newtonian–Newtonian). The deformation of a Newtonian droplet in a viscoelastic carrier fluid is ‘ellipsoid-like’ (Chung et al. 2008). Comparing to a Newtonian droplet, the deformation of a Non-Newtonian droplet is complicated. A comparison of deformations for a bubble and a capsule under confinement has been investigated in Ref. (Dawson et al. 2015).

A summary of relevant deformation and confinement evaluation parameter is given in Table 10. The Taylor deformation index is the most popular deformation index used to quantify the deformation of the dispersed phase. The DI changes with the flow and has a direct influence on cell fatigue (Sakuma et al. 2014). A droplet can support larger deformations than cells and solid particles due to its lack of elasticity.

The confinement index is defined as the dimension ratio of the un-deformed droplet and the constricted channel. Although defined in different forms, three confinement index listed in Table 10 is easily convertible.

6 Challenges

Four challenging problems are discussed in this chapter: complex dispersed phase, multiphysics process, modeling a cell under confinement, and processing rate.

6.1 Complex dispersed phases

A particle can be “complex” in its constitutive relation, flow condition (constricted), or structure. In comparison with the constitutive equation complexities, modeling of structurally complex disperse phases may be challenging numerically, while there are instability problems, such as in the droplet emulsion and droplet encapsulation, in the experiments. Comparison of complex dispersed phases is shown in Fig. 6.

A cluster is a group of particles. Interactions for clusters have been studied for the multiple-droplet cluster (Rosenfeld et al. 2014), CTC clusters (Au et al. 2016), RBCs/platelets cluster (Yazdani and Karniadakis 2016), and RBCs/microparticles cluster (Bächer et al. 2017) when flowing through a constricted channel. These researches have significance in understanding applications such as red blood cell aggregation, CTC cluster metastasis, or droplet emulsion.

A multiscale dispersed phase may have a very thin but functional layer/membrane such as a cell membrane or encapsulated layer. The dissipative particle dynamics (DPD) method is a particle-based numerical method (Li et al. 2014) that can be used in the study of the mechanical response of

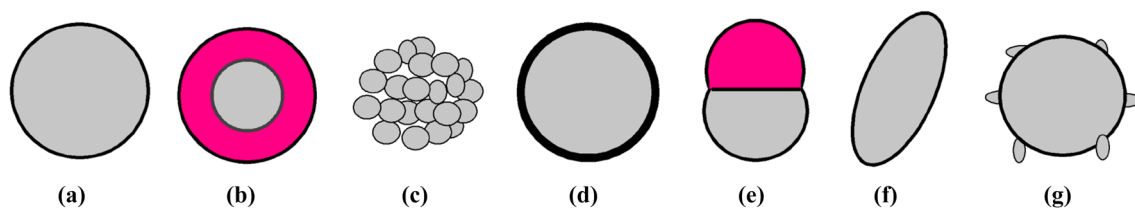


Fig. 6 Complex particle structure, **a** simple particle, **b** compound particle, **c** cell/particle cluster, **d** multiscale dispersed phase, **e** Janus structure, **f** non-spherical dispersed phase, and **g** active cell model. Color difference stands for a material difference. (Color figure online)

lipid bilayer, cytoskeleton under confinement. The numerical challenge of the modeling a multiscale cell will be discussed in Sect. 6.3.

Other types of complex particles also exist. Many cells are non-spherical, such as RBC, adhesive cells, or special capsules. Disks, rings, crosses, and S-shapes are other shape modes of particles (She et al. 2012). SPH method, LBM, front-tracking method, and the DPD method have been successfully applied to simulate non-spherical cells squeezed through channel confinements (Ye et al. 2016). Janus particles are composed of two-faced particles with distinctive surfaces and/or compartments. Studies of Janus particles under confinement have not been reported yet, possibly due to the instability of Janus droplets or a lack of real-life applications.

Furthermore, the models reviewed above were mainly passive deformable particles. However, cells are active, which are more complex. Self-propelled cells are closer to living cells (Lagny and Bassereau 2015). The cell under confinement problem will be discussed in Sect. 6.3.

6.2 Multiphysics process

6.2.1 Acoustic or oscillation

Acoustic and oscillation are pure mechanical forces. They have been proved to be bio-compatible. Under acoustic or vibration, a constricted channel can provide selective particle penetration.

Following are some studies that used the model of a particle under confinement in an acoustic field. For example, acoustic waves can facilitate oil motion or breakup in petroleum emulsion. The oscillatory pressure enables cell transport when the pressure amplitude and oscillation period exceed required threshold values. Results show that low-frequency oscillations can mobilize the residual oil droplets (Beresnev et al. 2005) and cells (Guo et al. 2011) better than higher frequency ones, or resulting in a higher cumulative forward motion. Oscillations at frequencies higher than the critical frequency almost nearly have no influence on the dispersed phase. The scattering caused by the confinement can lead to a discrepancy between numerical and analytical results. Two types of acoustic waves, square (Aghaamoo

et al. 2015) and saw-tooth (Myrand-Lapierre et al. 2015) pressure waveforms have been used in the squeezing of the dispersed phase. A summary of acoustic applications is given in Table 11.

6.2.2 Electric field

There are many applications based on the combined effect of the electronic field and channel confinement. For instance (as seen in Fig. 7)

- (a) Due to frictions at the channel wall, the droplet can be charged considerably during aspiration. The charge magnitude depends on the constituents of the droplet, environment, and operation condition. The charge may affect droplet detachment (Choi et al. 2013). Based on this finding, it is possible to quantify surface roughness of droplet-like cells through electrostatic or improve the roughness models towards more accurate cell property measurements.
- (b) A polarizable droplet can be obtained by applying an electric field. The surface tension coefficient of a liquid metal droplet can become non-uniform and voltage-dependent in an electric field. The change of the surface tension coefficient is proportional to the applied voltage squared. By adding an alternating electric current, the polarized droplet can enhance the micromixing by stirring the fluid through vibration (Hu et al. 2017).
- (c) When a cell in electric field flows through a constricted channel, an electronic current impulse can be observed (Zheng et al. 2012). By recognizing the impulse, the electronic property of a cell can be measured in a constricted channel (Zhao et al. 2015) or through automated micropipette aspiration (Shojaei-Baghini et al. 2013). The impedance profile of a cell can be used to classify cell types (Chen et al. 2011). However, for this measurement, the cell needs to be in good contact with the constricted channel. The carrier fluid leakage will deteriorate the electric conduction. Thus, the co-flow (the flow of the carrier fluid around cells or particles) is a physical limit of these applications.
- (d) In the droplet generation by liquid dielectrophoresis (DEP) actuation, two electrodes form a planar constricted

Table 11 Oscillation and constricted channel combined device

Confinement	Frequency (Hz)	Function	References
Circular pillar	75–225	Acoustic waves on the dissolution and mobilization dispersed phase	Chrysikopoulos and Vogler (2006)
Porous media	10, 30, and 60	Elastic waves in porous media with a porosity of 0.44	Beresnev et al. (2005)
Ratchet	0.33, 0.5, and 1	Selective cell transportation by oscillatory pressure	Guo et al. (2011)
CTC filter	666, 1333, 2666	Numerical design CTC filter using ratchet and square wave	Aghaamoo et al. (2015)

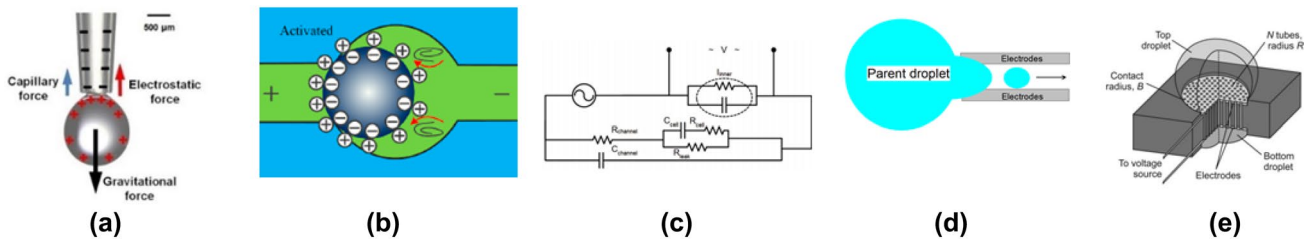


Fig. 7 (a) Electrostatic, experiment influence should be taken care of at small scales. Figure reproduced from (Choi et al. 2013). (b) Mixer under AC voltage. The charged liquid metal droplet plays the role of mixing enhancement. Figure reproduced from (Hu et al. 2017). (c) Cell property measurement. Figure reproduced from (Zheng et al. 2012) with permission from The Royal Society of Chemistry.

(d) Droplet generation by liquid dielectrophoresis (DEP) actuation (Ahmed and Jones 2007). Adapted with permission. ©IOP Publishing. All rights reserved. (e) Electroosmotic droplet switch. Reproduced from (Vogel et al. 2005). Copyright (2005) National Academy of Sciences, USA

Table 12 Hybrid algorithms developed in simulating a cell squeezing through a narrow confinement

Hybrid method		Function
BIM–FEM (Hu et al. 2012)	Boundary integral method	Internal and external fluid motion in a spherical capsule
	Finite-element method	Membrane deformation
LS-FEM (Roca and Carvalho 2013)	Level set	Interface tracking
	Finite-element method	Solve the momentum and mass conservation equations
LBM–IBM–FEM (Gounley et al. 2017)	Lattice Boltzmann Method	Solve carrier fluid on an Euler grid
	Finite-element method	Solver capsule membrane force on a Lagrangian grid
	Immersed boundary method	Couple the deformable capsules to the fluid field

tion. Precisely controlled-droplet dispensing can generate a droplet size ranges from ~ 10 pL to 100 nL. By rapid actuation of a droplet, the electric field can be used to control surface tension (Pollack et al. 2000). Particles can be trapped by DEP (Gencoglu et al. 2013).

(e) In the electroosmotic droplet switch, the capillarity is balanced by electrokinetics (Vogel et al. 2005). The moving droplet plays the role of an electromechanical transducer. However, the droplet evaporates and changes the property of the switch, which limits future applications.

6.2.3 Magnetic and other fields

Magnetic beads can guide or pull a cell/particle into a constricted channel to measure the cell membrane property (Liu et al. 2015) or help cell filtrations (Chang et al. 2014). Alternatively, the optofluidic approach (Vazquez et al. 2015) was also capable of transporting a cell through a narrow constriction. However, due to the limitation in effective power, the optic-based devices have seldom been used to operate large particles (> 20 μm), cell clusters, or tissue.

6.3 Modeling a cell under confinement

Tremendous efforts have been made in the modeling of a cell flow in a confinement. All models mentioned in the present review (droplet, solid particle including compound particle, multiscale particle, or other types of complex structure particles, capsule, and vesicle) have been used to model a cell.

When a cell is squeezed through a narrow-constricted channel, the cytoplasm and nucleus must deform. The nucleus is a physical barrier (McGregor et al. 2016), which increases the squeezing (Zhang et al. 2015) pressure. Simulating a compound droplet is computationally challenging due to continuous deformation of three phases: (1) the inner nucleus; (2) the fluid inside the cytoplasm; and (3) the carrier fluid (Zhou et al. 2008), and the continuous moving of two interfaces with complex wettability (Blunt 2001; Hui and Blunt 2000).

As reviewed in a previous section, each numerical method has advantages and limitations. To solve complex numerical problems, hybrid methods have been developed such as level set-IBM method (Cottet and Maitre 2004) and immersed interface method (Sethian and Wiegmann 2000), and LBM–IBM (Bächer et al. 2017) (see Table 12). Hybrid algorithms developed to simulate the multiscale effect in a cell were summarized in the following table. In these hybrid

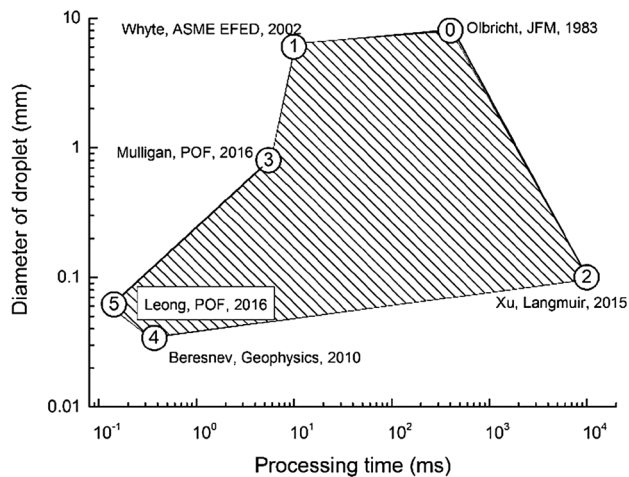


Fig. 8 Processing time (x -axis) and droplet diameter (y -axis) for droplet emulsion and break-up using a constricted channel

algorithms, the immersed boundary method (IBM) is often employed to model the coupling between fluid and solid (Tan et al. 2018a, b).

There are two main challenges in modeling a cell in confinement:

1. The mechanism of active forces is still challenging and unsolved. The Osmotic Engine Model can predict the active cell migration in a confined channel. In this model, the active force was generated by net water flow pumping through transmembrane proteins (Stroka et al. 2014). Recently, a numerical model of an active vesicle transportation model was proposed to understand how active force transports a cell through a blind constricted channel (Fai et al. 2017). In this model, the effective propulsion force is generated by molecular motors in the lubrication zone in the membrane. The model can capture different behaviors of an active cell such as vesicle rejection, corking, and translocation (Fai et al. 2017).
2. Multiscale structures in a cell are complex. The response of a cell under confinement is important in pathology. The dissipative particle dynamics (DPD method) can simulate thin lipid bilayer and the cytoskeleton (Peng et al. 2013). In the cell squeezing problem (Pivkin et al. 2016), fluid-induced membrane tension is large enough to overcome cytoskeleton resistance and opens the mechanosensitive gates, which allow the transportation of large molecules (Pak et al. 2015). The coarse-grained multiscale method proposed by Zhang et al. (2015a, b, c) and the phase-field multiscale method proposed by Peco et al. (2017) can potentially be used to simulate the features of cell membrane gating or bilayer cracking in the process of cell squeezing problem. However, all these efforts are towards the mechanical properties of cells,

and more complicated chemical process and biological process have not been investigated. Towards whole-cell modeling, complex software platform called “E-cell”, targeting at simulating a real cell including gene, has been developed over 20 years (Tomita et al. 1999). To the best of authors’ knowledge, the multiscale modeling of the E-cell under confinement problem has not been conducted, which is extremely challenging. The model of a particle squeezed through a constricted channel has been used as standard testing for material properties and is becoming a standard benchmark for numerical cell models (Peng et al. 2013).

6.4 High-processing rate

High throughput is required in batch-processing applications of droplets and cells. Examples of batch processing using fluid dynamics (Zhao et al. 2016) include droplet emulsion, property measurement, cell labeling, cell filtration, etc. For the droplet emulsion in a constricted channel, we collected from literature drop’s diameters, processing times, and publications. These data are schematically represented in Fig. 8 with the processing time as the x -axis and the size of the droplet as the y -axis. Since the first published application in 1983, more work has been conducted in the emulsion of droplets at a higher speed (marked as odd numbers) and smaller size (marked as even numbers). Most droplet breakup and emulsion applications are within the region shown in Fig. 8. From this figure, we can see a trend of a quicker processing rate requirement for smaller droplets. Alternatively, for cell applications, the deformability measurement is usually at the level of 10 cells/min (Monzawa et al. 2015) (Hoelzle et al. 2014) up to 100 cells through multi-sample devices (Ahmmed et al. 2018a, b), while the separation of cells at a level up to hundreds of cells/min (Lin et al. 2013). In applications of macromolecular or drug delivery, the processing rate can reach up to 25,000 cells/s (Sharei et al. 2013), or higher in the protein labeling application (Kollmannsperger et al. 2016).

7 Summary

This paper reviewed recent progress in the applications, modeling, physics, and design of narrow confinements for the manipulation of a droplet, cell, and solid particle. Although many advanced multiphysics tools have been developed for particle manipulation, the constricted channel continues to be widely used thanks to its simplicity and versatility. However, we found most researchers focused on their own applications with limited reference to the same model in other research backgrounds. Through the review, we intent to bring researchers from different fields together

and find common problems through recent fast growing literature.

1. In applications, a historical view shows that the particle-squeezing model has broad applications across macro-, meso-, or microscale problems since 40 years ago. Recent applications in biomedical, pathology, and clinical trials inspired most of the recent research. Many new phenomena have been observed in the applications of the model, in multiscale or multiphysics research interests.
2. Although technically challenging, several large-scale numerical models in simulating interactions in particle clusters, porous media, or multiscale cell models have been developed. Due to resource consuming and no open-source environment, many numerical codes are not easily accessible to most researchers. Furthermore, due to the problem's nature as time dependent, multiphase flow, multiple control parameters, or even multiphysics fields, the research in the physics and optimization of the model progressed slowly and remains open problems.
3. Quantitative mathematical descriptions that can relate the particle deformation behavior with material properties, flow conditions, and geometries remain challenging and have not been developed yet. Insufficient efforts were engaged in developing analytical models for particle deformation, stress/strain, or instability problems. For examples, although the Young–Laplace equation was found problematic in high-flowrate operations or a cell-squeezing cases, it is still the most widely used design criteria due to lack of more precise descriptions. Similarly, the analytical expression for the transient squeezing pressure is still unsolved for the straightforward case such as a two-component droplet squeezing (with surface tension and viscosity).

Acknowledgements Zhifeng Zhang thanks the support of Harvey & Geraldine Brush Fellowship and Max & Joan Schlienger Scholarship awarded by College of Engineering, the Pennsylvania State University.

References

- Abkarian M, Faivre M, Horton R, Smistrup K, Best-Popescu CA, Stone HA (2008) Cellular-scale hydrodynamics. *Biomed Mater* 3:034011
- Aceto N et al (2014) Circulating tumor cell clusters are oligoclonal precursors of breast cancer metastasis. *Cell* 158:1110–1122
- Aghaamoo M, Zhang Z, Chen X, Xu J (2015) Deformability-based circulating tumor cell separation with conical-shaped microfilters: concept, optimization, and design criteria. *Biomicrofluidics* 9:034106
- Ahmed R, Jones T (2007) Optimized liquid DEP droplet dispensing. *J Micromech Microeng* 17:1052
- Ahmed SM, Bithi SS, Pore AA, Muhtasim N, Schuster C, Gol-lahon LS, Vanapalli SA (2018a) Multi-sample deformability cytometry of cancer cells. *APL Bioeng* 2:032002
- Ahmed SM, Suteria NS, Garbin V, Vanapalli SA (2018b) Hydrodynamic mobility of confined polymeric particles, vesicles, and cancer cells in a square microchannel. *Biomicrofluidics* 12:014114
- Alix-Panabières C, Pantel K (2014) Technologies for detection of circulating tumor cells: facts and vision. *Lab Chip* 14:57–62
- Anselmo A, Mitragotri S (2016) Designing drug-delivery nanoparticles. *Chem Eng Prog* 112: 52–57
- Aoki T, Ohashi T, Matsumoto T, Sato M (1997) The pipette aspiration applied to the local stiffness measurement of soft tissues. *Ann Biomed Eng* 25:581–587
- Arata JP, Alexeev A (2009) Designing microfluidic channel that separates elastic particles upon stiffness. *Soft Matter* 5:2721–2724
- Argatov I, Mishuris G (2016) Pipette aspiration testing of soft tissues: the elastic half-space model revisited. In: *Proc. R. Soc. A*, vol 2193. The Royal Society, p 20160559
- Au SH et al (2016) Clusters of circulating tumor cells traverse capillary-sized vessels. *Proc Natl Acad Sci* 113:4947–4952
- Ayan B et al (2017) A new aspiration-assisted bioprinting method for tissue fabrication. Paper presented at the Symposium on Biomaterials Science, New Jersey, USA
- Bächer C, Schrack L, Gekle S (2017) Clustering of microscopic particles in constricted blood flow. *Phys Rev Fluids* 2:013102
- Barakat JM, Shaqfeh ESG (2018) The steady motion of a closely fitting vesicle in a tube. *J Fluid Mech* 835:721–761
- Barthès-Biesel D (2012) *Microhydrodynamics and complex fluids*. CRC Press, Boca Raton
- Beckman S, Barbano D (2013) Effect of microfiltration concentration factor on serum protein removal from skim milk using spiral-wound polymeric membranes. *J Dairy Sci* 96:6199–6212
- Benet E, Vernerey F (2016) Mechanics and stability of vesicles and droplets in confined spaces. *Phys Rev E* 94:062613
- Benet E, Badran A, Pellegrino J, Vernerey F (2017) The porous media's effect on the permeation of elastic (soft) particles. *J Membr Sci* 535:10–19
- Beresnev IA, Deng W (2010) Viscosity effects in vibratory mobilization of residual oil. *Geophysics* 75:N79–N85
- Beresnev IA, Vigil RD, Li W, Pennington WD, Turpening RM, Iasonov PP, Ewing RP (2005) Elastic waves push organic fluids from reservoir rock. *Geophys Res Lett* 32
- Beresnev IA, Li W, Vigil RD (2009) Condition for break-up of non-wetting fluids in sinusoidally constricted capillary channels. *Transp Porous Media* 80:581–604
- Beresnev I, Gaul W, Vigil RD (2011) Direct pore-level observation of permeability increase in two-phase flow by shaking. *Geophys Res Lett* 38:L20302
- Berthier J, Brakke K (2012) *The physics of microdroplets*. Wiley, Hoboken
- Bindiganavale GS, Moon H, You SM, Amaya M (2012) Digital microfluidic device for hotspot cooling in ICS using electrowetting on dielectric. Paper presented at the ASME 2012 third international conference on micro/nanoscale heat and mass transfer
- Bindiganavale G, You SM, Moon H (2014) Study of hotspot cooling using electrowetting on dielectric digital microfluidic system. Paper presented at the Micro Electro Mechanical Systems (MEMS), 2014 IEEE 27th International Conference on
- Blakely AM, Manning KL, Tripathi A, Morgan JR (2015) Bio-pick, place, and perfuse: a new instrument for three-dimensional tissue engineering. *Tissue Eng Part C Methods* 21:737–746
- Blunt MJ (2001) Flow in porous media-pore-network models and multiphase flow. *Curr Opin Colloid Interface Sci* 6:197–207

- Boukellal H, Selimovic S, Jia Y, Cristobal G, Fraden S (2009) Simple, robust storage of drops and fluids in a microfluidic device. *Lab Chip* 9:331–338
- Bow H et al (2011) A microfabricated deformability-based flow cytometer with application to malaria. *Lab Chip* 11:1065–1073
- Brakke KA (1992) The surface evolver. *Exp Math* 1:141–165
- Brosseau Q, Vrignon J, Baret J-C (2014) Microfluidic dynamic interfacial tensiometry (μ DIT). *Soft Matter* 10:3066–3076
- Brouzes E et al (2009) Droplet microfluidic technology for single-cell high-throughput screening. *Proc Natl Acad Sci* 106:14195–14200
- Byun S et al (2013) Characterizing deformability and surface friction of cancer cells. *Proc Natl Acad Sci* 110:7580–7585
- Casquero H, Bona-Casas C, Gomez H (2017) NURBS-based numerical proxies for red blood cells and circulating tumor cells in microscale blood flow. *Comput Methods Appl Mech Eng* 316:646–667
- Chang C-L, Jalal SI, Huang W, Mahmood A, Matei DE, Savran CA (2014) High-throughput immunomagnetic cell detection using a microaperture chip system. *IEEE Sens J* 14:3008–3013
- Chen H, Zhang Z (2018) An inertia-deformability hybrid circulating tumor cell chip: design, clinical test, and numerical analysis. *J Med Devices* 12(4):041004
- Chen J et al (2011) Classification of cell types using a microfluidic device for mechanical and electrical measurement on single cells. *Lab Chip* 11:3174–3181
- Chen Y et al (2014) Rare cell isolation and analysis in microfluidics. *Lab Chip* 14:626–645
- Chen H, Cao B, Sun B, Cao Y, Yang K, Lin Y-S, Chen H (2017a) Highly-sensitive capture of circulating tumor cells using micro-ellipse filters. *Sci Rep* 7:610
- Chen L, Wang KX, Doyle PS (2017b) Effect of internal architecture on microgel deformation in microfluidic constrictions. *Soft Matter* 13:1920–1928
- Chiu J-J, Chien S (2011) Effects of disturbed flow on vascular endothelium: pathophysiological basis and clinical perspectives. *Physiol Rev* 91:327–387
- Choi D, Lee H, Im DJ, Kang IS, Lim G, Kim DS, Kang KH (2013) Spontaneous electrical charging of droplets by conventional pipetting. *Scientific Reports* 3:2037
- Christafakis AN, Tsangaris S (2008) Two-phase flows of droplets in contractions and double bends. *Eng Appl Comput Fluid Mech* 2:299–308
- Chrysikopoulos CV, Vogler ET (2006) Acoustically enhanced ganglia dissolution and mobilization in a monolayer of glass beads. *Transp Porous Media* 64:103–121
- Chung C, Hulsen MA, Kim JM, Ahn KH, Lee SJ (2008) Numerical study on the effect of viscoelasticity on drop deformation in simple shear and 5: 1: 5 planar contraction/expansion microchannel. *J Nonnewton Fluid Mech* 155:80–93
- Chung C, Lee M, Char K, Ahn KH, Lee SJ (2010) Droplet dynamics passing through obstructions in confined microchannel flow. *Microfluid Nanofluid* 9:1151–1163
- Clark S, Haubert K, Beebe DJ, Ferguson E, Wheeler M (2005) Reduction of polyspermic penetration using biomimetic microfluidic technology during in vitro fertilization. *Lab Chip* 5:1229–1232
- Comanns P, Buchberger G, Buchsbaum A, Baumgartner R, Kogler A, Bauer S, Baumgartner W (2015) Directional, passive liquid transport: the Texas horned lizard as a model for a biomimetic ‘liquid diode’. *J R Soc Interface* 12:20150415
- Cottet G-H, Maitre E (2004) A level-set formulation of immersed boundary methods for fluid–structure interaction problems. *CR Math* 338:581–586
- Danielczok JG, Terriac E, Hertz L, Petkova-Kirova P, Lautenschläger F, Laschke MW, Kaestner L (2017) Red blood cell passage of small capillaries is associated with transient Ca^{2+} -mediated adaptations. *Front Physiol* 8: 979
- Darvishzadeh T, Priezjev NV (2012) Effects of crossflow velocity and transmembrane pressure on microfiltration of oil-in-water emulsions. *J Membr Sci* 423–424:468–476
- Datta P, Ayan B, Ozbolat IT (2017) Bioprinting for vascular and vascularized tissue biofabrication. *Acta Biomater* 51:1–20
- Dawson G, Häner E, Juel A (2015) Extreme deformation of capsules and bubbles flowing through a localised constriction. *Proc IUTAM* 16:22–32
- Dixon MW, Dearnley MK, Hanssen E, Gilberger T, Tilley L (2012) Shape-shifting gametocytes: how and why does *P. falciparum* go banana-shaped? *Trends Parasitol* 28:471–478
- Dressaire E, Sauret A (2017) Clogging of microfluidic systems. *Soft Matter* 13:37–48
- Drury J, Dembo M (1999) Hydrodynamics of micropipette aspiration. *Biophys J* 76:110–128
- Drury J, Dembo M (2001) Aspiration of human neutrophils: effects of shear thinning and cortical dissipation. *Biophys J* 81:3166–3177
- Evans EA, Waugh R, Melnik L (1976) Elastic area compressibility modulus of red cell membrane. *Biophys J* 16:585–595
- Fabbri F et al (2013) Detection and recovery of circulating colon cancer cells using a dielectrophoresis-based device: KRAS mutation status in pure CTCs. *Cancer Lett* 335:225–231
- Facchin S, Miled MA, Sawan M (2015) In-channel constriction valve for cerebrospinal fluid sampling. *IEEE Trans Magn* 51:1–4
- Fai T, Kusters R, Harting J, Rycroft C, Mahadevan L (2017) Active elasto-hydrodynamics of vesicles in narrow, blind constrictions. *arXiv preprint arXiv:170501765*
- Fang Z, Zhang Z, Chen X, Xu J (2014) Inertial microfluidic spiral CTCs filter with micropillars. Paper presented at the 36th EMBS special topic conference on healthcare innovation & point-of-care technologies, Seattle, WA, USA
- Fenton B, Wilson D, Cokelet G (1985) Analysis of the effects of measured white blood cell entrance times on hemodynamics in a computer model of a microvascular bed. *Pflügers Arch* 403:396–401
- Fischer-Friedrich E, Hyman AA, Jülicher F, Müller DJ, Helenius J (2014) Quantification of surface tension and internal pressure generated by single mitotic cells. *Sci Rep* 4:6213
- Frostad JM, Paul A, Leal LG (2016) Coalescence of droplets due to a constant force interaction in a quiescent viscous fluid. *Phys Rev Fluids* 1:033904
- Gai Y, Khor JW, Tang S (2016) Confinement and viscosity ratio effect on droplet break-up in a concentrated emulsion flowing through a narrow constriction. *Lab Chip* 16:3058–3064
- Gencoglu A, Olney D, LaLonde A, Koppula K, Lapizco-Encinas B (2013) Particle manipulation in insulator based dielectrophoretic devices. *J Nanotechnol Eng Med* 4:021002–021002
- Genovese D, Sprakel J (2011) Crystallization and intermittent dynamics in constricted microfluidic flows of dense suspensions. *Soft Matter* 7:3889–3896
- Gounley J, Draeger EW, Randles A (2017) Numerical simulation of a compound capsule in a constricted microchannel. *Proc Comput Sci* 108:175–184
- Guevorkian K, Colbert M-J, Durth M, Dufour S, Brochard-Wyart F (2010) Aspiration of biological viscoelastic drops. *Phys Rev Lett* 104:218101
- Guilak F, Tedrow JR, Burgkart R (2000) Viscoelastic properties of the cell nucleus. *Biochem Biophys Res Commun* 269:781–786
- Guo Q, Ma H (2011) Microfluidic device for measuring the stiffness of single cells. In: 15th International Conference on Miniaturized Systems for Chemistry and Life Sciences, 2–6 October 2011, Seattle, Washington, USA
- Guo Q, McFaul SM, Ma H (2011) Deterministic microfluidic ratchet based on the deformation of individual cells. *Phys Rev E* 83:051910

- Guo Q, Park S, Ma H (2012) Microfluidic micropipette aspiration for measuring the deformability of single cells. *Lab Chip* 12:2687–2695
- Guo Q, Duffy SP, Matthews K, Deng X, Santoso AT, Islamzada E, Ma H (2016) Deformability based sorting of red blood cells improves diagnostic sensitivity for malaria caused by *Plasmodium falciparum*. *Lab Chip* 16:645–654
- Gupta A, Matharoo HS, Makkar D, Kumar R (2014) Droplet formation via squeezing mechanism in a microfluidic flow-focusing device. *Comput Fluids* 100:218–226
- Haider MA, Guilak F (2002) An axisymmetric boundary integral model for assessing elastic cell properties in the micropipette aspiration contact problem. *J Biomech Eng* 124:586–595
- Han X et al (2015) CRISPR-Cas9 delivery to hard-to-transfect cells via membrane deformation. *Sci Adv* 1:e1500454
- Harvie D, Cooper-White J, Davidson M (2008) Deformation of a viscoelastic droplet passing through a microfluidic contraction. *J Nonnewton Fluid Mech* 155:67–79
- Hassanzadeh A, Pourmahmoud N, Dadvand A (2017) Numerical simulation of motion and deformation of healthy and sick red blood cell through a constricted vessel using hybrid lattice Boltzmann-immersed boundary method. *Comput Methods Biomech Biomed Eng* 20:1–13
- Hendrickson GR, Lyon LA (2010) Microgel translocation through pores under confinement. *Angew Chem Int Ed* 49:2193–2197
- Herant M, Heinrich V, Dembo M (2005) Mechanics of neutrophil phagocytosis: behavior of the cortical tension. *J Cell Sci* 118:1789–1797
- Hochmuth RM (2000) Micropipette aspiration of living cells. *J Biomech* 33:15–22
- Hoelzle D, Varghese B, Chan C, Rowat A (2014) A microfluidic technique to probe cell deformability. *J Vis Exp* 91:e51474
- Hong B, Zu Y (2013) Detecting circulating tumor cells: current challenges and new trends. *Theranostics* 3:377–396
- Hu X, Salsac A, Barthès-Biesel D (2012) Flow of a spherical capsule in a pore with circular or square cross-section. *J Fluid Mech* 705:176–194
- Hu Q, Ren Y, Liu W, Chen X, Tao Y, Jiang H (2017) Fluid flow and mixing induced by AC continuous electrowetting of liquid metal droplet. *Micromachines* 8:119
- Hua H, Shin J, Kim J (2014) Dynamics of a compound droplet in shear flow. *Int J Heat Fluid Flow* 50:63–71
- Hui M-H, Blunt MJ (2000) Effects of wettability on three-phase flow in porous media. *J Phys Chem B* 104:3833–3845
- Ito H et al (2017) Mechanical diagnosis of human erythrocytes by ultra-high speed manipulation unraveled critical time window for global cytoskeletal remodeling. *Scientific Reports* 7: 43134
- Izbassarov D, Muradoglu M (2016) A computational study of two-phase viscoelastic systems in a capillary tube with a sudden contraction/expansion. *Phys Fluids* 28:012110
- Kadivar E, Farrokhbin M (2017) A numerical procedure for scaling droplet deformation in a microfluidic expansion channel. *Phys A* 479:449–459
- Kan H-C, Udaykumar H, Shyy W, Tran-Son-Tay R (1998) Hydrodynamics of a compound drop with application to leukocyte modeling. *Phys Fluids* 10:760–774
- Khalifat N, Beaune G, Nagarajan U, Winnik FM, Brochard-Wyart F (2016) Soft matter physics: Tools and mechanical models for living cellular aggregates. *Jpn J Appl Phys* 55:1102A1108
- Khambhampati TK (2013) A comparative study between Newtonian and non-Newtonian models in a stenosis of a carotid artery. Master Thesis. Texas A&M University, College Station
- Kim M-Y, Oskarsson T, Acharyya S, Nguyen DX, Zhang XH-F, Norton L, Massague J (2009) Tumor self-seeding by circulating cancer cells. *Cell* 139:1315–1326
- Kim Y, Kim K, Park Y (2012) Measurement techniques for red blood cell deformability: recent advances. INTECH Open Access Publisher Rijeka, Croatia
- Kim J, Lee H, Shin S (2015) Advances in the measurement of red blood cell deformability: a brief review. *J Cell Biotechnol* 1:63–79
- Kollmannsperger A et al (2016) Live-cell protein labelling with nanometre precision by cell squeezing. *Nat Commun* 7:10372
- Kong T, Wang L, Wyss HM, Shum HC (2014) Capillary micromechanics for core-shell particles. *Soft Matter* 10:3271–3276
- Kusters R, van der Heijden T, Kaoui B, Harting J, Storm C (2014) Forced transport of deformable containers through narrow constrictions. *Phys Rev E* 90:033006
- Lagny TJ, Bassereau P (2015) Bioinspired membrane-based systems for a physical approach of cell organization and dynamics: usefulness and limitations. *Interface Focus* 5:20150038
- Lange JR, Steinwachs J, Kolb T, Lautscham LA, Harder I, Whyte G, Fabry B (2015) Microconstriction arrays for high-throughput quantitative measurements of cell mechanical properties. *Biophys J* 109:26–34
- Lautscham LA et al (2015) Migration in confined 3D environments is determined by a combination of adhesiveness, nuclear volume, contractility, and cell stiffness. *Biophys J* 109:900–913
- Lazaro GR, Hernandez-Machado A, Pagonbarraga I (2014) Rheology of red blood cells under flow in highly confined microchannels. II. Effect of focusing and confinement. *Soft Matter* 10:7207–7217
- Le Goff A, Kaoui B, Kurzawa G, Haszon B, Salsac A-V (2017) Squeezing bio-capsules into a constriction: deformation till break-up. *Soft Matter* 13:7644–7648
- Lee MS (2010) Computational studies of droplet motion and deformation in a microfluidic channel with a constriction. Master Thesis, University of Maryland, College Park, USA
- Lee L, Liu A (2014) The application of micropipette aspiration in molecular mechanics of single cells. *J Nanotechnol Eng Med* 5:040902
- Lee G-H, Kim S-H, Ahn K, Lee S-H, Park JY (2015) Separation and sorting of cells in microsystems using physical principles. *J Micromech Microeng* 26:013003
- Legait B (1983) Laminar flow of two phases through a capillary tube with variable square cross-section. *J Colloid Interface Sci* 96:28–38
- Legait B, Sourieau P, Combarous M (1983) Inertia, viscosity, and capillary forces during two-phase flow in a constricted capillary tube. *J Colloid Interface Sci* 91:400–411
- Leong FY, Li Q, Lim CT, Chiam K-H (2011) Modeling cell entry into a micro-channel. *Biomech Model Mechanobiol* 10:755–766
- Li H (2010) Smart hydrogel modelling. Springer, Berlin
- Li X, Peng Z, Lei H, Dao M, Karniadakis GE (2014) Probing red blood cell mechanics, rheology and dynamics with a two-component multi-scale model. *Philos Trans R Soc Lond A Math Phys Sci* 372:20130389
- Li Y, Sariyer OS, Ramachandran A, Panyukov S, Rubinstein M, Kumacheva E (2015) Universal behavior of hydrogels confined to narrow capillaries. *Sci Rep* 5: 17017
- Li H, Chen J, Du W, Xia Y, Wang D, Zhao G, Chu J (2017) The optimization of a microfluidic CTC filtering chip by simulation. *Micromachines* 8:79
- Liang M, Yang S, Miao T, Yu B (2015) Minimum applied pressure for a drop through an abruptly constricted capillary. *Microfluid Nanofluidics* 19:1–8
- Lin BK, McFaul SM, Jin C, Black PC, Ma H (2013) Highly selective biomechanical separation of cancer cells from leukocytes using microfluidic ratchets and hydrodynamic concentrator. *Biomicrofluidics* 7:034114
- Liu F, KC P, Zhang G, Zhe J (2015) Microfluidic magnetic bead assay for cell detection. *Anal Chem* 88:711–717

- Lorenceanu É, Quéré D (2003) Drops impacting a sieve. *J Colloid Interface Sci* 263:244–249
- Luo Z, Bai B (2017) Off-center motion of a trapped elastic capsule in a microfluidic channel with a narrow constriction. *Soft Matter* 13:8281–8292
- Luo Z, Bai B (2018) Dynamics of capsules enclosing viscoelastic fluid in simple shear flow. *J Fluid Mech* 840:656–687
- Luo Y et al (2014) A constriction channel based microfluidic system enabling continuous characterization of cellular instantaneous Young's modulus. *Sens Actuators B* 202:1183–1189
- Luo Z et al (2015) Deformation of a single mouse oocyte in a constricted microfluidic channel. *Microfluid Nanofluidics* 19:883–890
- Marella S, Udaykumar H (2004) Computational analysis of the deformability of leukocytes modeled with viscous and elastic structural components. *Phys Fluids* 16:244–264
- Massenburg SS, Amstad E, Weitz DA (2016) Clogging in parallelized tapered microfluidic channels. *Microfluid Nanofluid* 20:1–5
- McGregor AL, Hsia C-R, Lammerding J (2016) Squish and squeeze—the nucleus as a physical barrier during migration in confined environments. *Curr Opin Cell Biol* 40:32–40
- Middleman S (1995) Modeling axisymmetric flows: dynamics of films, jets, and drops. Academic Press, New York
- Mittal R, Simmons S, Najjar F (2003) Numerical study of pulsatile flow in a constricted channel. *J Fluid Mech* 485:337–378
- Mogensen K, Stenby EH (1998) A dynamic two-phase pore-scale model of imbibition. *Transp Porous Media* 32:299–327
- Monzawa T, Kaneko M, Tsai C-HD, Sakuma S, Arai F (2015) On-chip actuation transmitter for enhancing the dynamic response of cell manipulation using a macro-scale pump. *Biomicrofluidics* 9:014114
- Mulligan MK, Rothstein JP (2011) The effect of confinement-induced shear on drop deformation and breakup in microfluidic extensional flows. *Phys Fluids* 23:022004
- Muradoglu M, Gokaltun S (2005) Implicit multigrid computations of buoyant drops through sinusoidal constrictions. *J Appl Mech* 71:857–865
- Myrand-Lapierre M-E, Deng X, Ang RR, Matthews K, Santoso AT, Ma H (2015) Multiplexed fluidic plunger mechanism for the measurement of red blood cell deformability. *Lab Chip* 15:159–167
- Olbricht W, Leal L (1983) The creeping motion of immiscible drops through a converging/diverging tube. *J Fluid Mech* 134:329–355
- Olgac U, Kayaalp AD, Muradoglu M (2006) Buoyancy-driven motion and breakup of viscous drops in constricted capillaries. *Int J Multiph Flow* 32:1055–1071
- Pak OS, Young Y-N, Marple GR, Veerapaneni S, Stone HA (2015) Gating of a mechanosensitive channel due to cellular flows. *Proc Natl Acad Sci* 112:9822–9827
- Park S-Y, Dimitrakopoulos P (2013) Transient dynamics of an elastic capsule in a microfluidic constriction. *Soft matter* 9:8844–8855
- Park S-Y, Nam Y (2017) Single-sided digital microfluidic (SDMF) devices for effective coolant delivery and enhanced two-phase cooling. *Micromachines* 8:3
- Pawar A, Caggioni M, Ergun R, Hartel R, Spicer P (2011) Arrested coalescence in Pickering emulsions. *Soft Matter* 7:7710–7716
- Peco C, Chen W, Liu Y, Bandi M, Dolbow JE, Fried E (2017) Influence of surface tension in the surfactant-driven fracture of closely-packed particulate monolayers. *Soft matter* 13:5832–5841
- Pegoraro C et al (2014) Translocation of flexible polymersomes across pores at the nanoscale. *Biomaterials Science* 2:680–692
- Peng Z, Li X, Pivkin IV, Dao M, Karniadakis GE, Suresh S (2013) Lipid bilayer and cytoskeletal interactions in a red blood cell. *Proc Natl Acad Sci* 110:13356–13361
- Pivkin I, Peng Z, Karniadakis G, Buffet P, Dao M, Suresh S (2016) Biomechanics of red blood cells in human spleen and consequences for physiology and disease. *Proc Natl Acad Sci* 113:7804–7809
- Pollack MG, Fair RB, Shenderov AD (2000) Electrowetting-based actuation of liquid droplets for microfluidic applications. *Appl Phys Lett* 77:1725–1726
- Prévost C, Zhao H, Manzi J, Lemichez E, Lappalainen P, Callan-Jones A, Bassereau P (2015) IRSp53 senses negative membrane curvature and phase separates along membrane tubules. *Nat Commun* 6:8529
- Ralf S, Martin B, Thomas P, Stephan H (2012) Droplet based microfluidics. *Rep Prog Phys* 75:016601
- Ratcliffe T, Zinchenko AZ, Davis RH (2010) Buoyancy-induced squeezing of a deformable drop through an axisymmetric ring constriction. *Phys Fluids* 22:082101
- Ratcliffe T, Zinchenko A, Davis R (2012) Simulations of gravity-induced trapping of a deformable drop in a three-dimensional constriction. *J Colloid Interface Sci* 383:167–176
- Ren X, Ghassemi P, Babahosseini H, Strobl JS, Agah M (2017) Single-cell mechanical characteristics analyzed by multiconstriction microfluidic channels. *ACS Sens* 2:290–299
- Roca J, Carvalho M (2013) Flow of a drop through a constricted microcapillary. *Comput Fluids* 87:50–56
- Rosenfeld L, Fan L, Chen Y, Swoboda R, Tang S (2014) Break-up of droplets in a concentrated emulsion flowing through a narrow constriction. *Soft Matter* 10:421–430
- Sakuma S, Kuroda K, Tsai C-HD, Fukui W, Arai F, Kaneko M (2014) Red blood cell fatigue evaluation based on the close-encountering point between extensibility and recoverability. *Lab Chip* 14:1135–1141
- Sarioglu AF et al (2015) A microfluidic device for label-free, physical capture of circulating tumor cell clusters. *Nature methods* 12:685
- Schebarchov D, Hendsy S (2011) Uptake and withdrawal of droplets from carbon nanotubes. *Nanoscale* 3:134–141
- Sendekie ZB, Gaveau A, Lammertink RGH, Bacchin P (2016) Bacteria delay the jamming of particles at microchannel bottlenecks. *Sci Rep* 6:31471
- Sethian JA, Wiegmann A (2000) Structural boundary design via level set and immersed interface methods. *J Comput Phys* 163:489–528
- Sharei A et al (2013) A vector-free microfluidic platform for intracellular delivery. *Proc Natl Acad Sci* 110:2082–2087
- She S, Xu C, Yin X, Tong W, Gao C (2012) Shape deformation and recovery of multilayer microcapsules after being squeezed through a microchannel. *Langmuir* 28:5010–5016
- Shelby JP, White J, Ganesan K, Rathod PK, Chiu DT (2003) A microfluidic model for single-cell capillary obstruction by Plasmodium falciparum-infected erythrocytes. *Proc Natl Acad Sci* 100:14618–14622
- Shen F, Pompano RR, Kastrup CJ, Ismagilov RF (2009) Confinement regulates complex biochemical networks: initiation of blood clotting by “diffusion acting”. *Biophysical journal* 97:2137–2145
- Shirai A, Masuda S (2013) Numerical simulation of passage of a neutrophil through a rectangular channel with a moderate constriction. *PLOS One* 8:e59416
- Shirai A, Fujita R, Hayase T (2002) Transit characteristics of a neutrophil passing through a circular constriction in a cylindrical capillary vessel. *JSME Int J Ser C Mech Syst Mach Elem Manuf* 45:974–980
- Shirai A, Fujita R, Hayase T (2003) Transit characteristics of a neutrophil passing through two moderate constrictions in a cylindrical capillary vessel. *JSME Int J Ser C Mech Syst Mach Elem Manuf* 46:1198–1207
- Shojaei-Baghini E, Zheng Y, Sun Y (2013) Automated micropipette aspiration of single cells. *Ann Biomed Eng* 41:1208–1216
- Shou D, Fan J (2015) Structural optimization of porous media for fast and controlled capillary flows. *Phys Rev E* 91:053021

- Shou D, Fan J (2018) Design of nanofibrous and microfibrillar channels for fast capillary flow. *Langmuir* 34:1235–1241
- Shou D, Ye L, Fan J, Fu K (2013) Optimal design of porous structures for the fastest liquid absorption. *Langmuir* 30:149–155
- Shou D, Ye L, Fan J, Fu K, Mei M, Wang H, Chen Q (2014a) Geometry-induced asymmetric capillary flow. *Langmuir* 30:5448–5454
- Shou D, Ye L, Fan J (2014b) The fastest capillary flow under gravity. *Appl Phys Lett* 104:231602
- Shou D, Ye L, Fan J (2014c) Treelike networks accelerating capillary flow. *Phys Rev E* 89:053007
- Sohrabi S, Tan J, Yunus DE, He R, Liu YJB (2018) Label-free sorting of soft microparticles using a bioinspired synthetic cilia array. *Biomicrofluidics* 12:042206
- Stewart MP, Sharei A, Ding X, Sahay G, Langer R, Jensen KF (2016) In vitro and ex vivo strategies for intracellular delivery. *Nature* 538:183–192
- Stroka KM, Jiang H, Chen S-H, Tong Z, Wirtz D, Sun SX, Konstantopoulos K (2014) Water permeation drives tumor cell migration in confined microenvironments. *Cell* 157:611–623
- Sun N, Li X, Wang Z, Li Y, Pei R (2018) High-purity capture of CTCs based on micro-beads enhanced isolation by size of epithelial tumor cells (ISET) method. *Biosens Bioelectr* 102:157–163
- Tan H (2016) Three-dimensional simulation of micrometer-sized droplet impact and penetration into the powder bed. *Chem Eng Sci* 153:93–107
- Tan J, Sinno TR, Diamond SL (2018a) A parallel fluid–solid coupling model using LAMMPS and Palabos based on the immersed boundary method. *J Comput Sci* 25:89–100
- Tan J, Sohrabi S, He R, Liu Y (2018b) Numerical simulation of cell squeezing through a micropore by the immersed boundary method. *Proc Inst Mech Eng Part C J Mech Eng Sci* 232:502–514
- Tasoglu S, Kaynak G, Szeri AJ, Demirci U, Muradoglu M (2010) Impact of a compound droplet on a flat surface: a model for single cell epitaxy. *Phys Fluids* 22:082103
- Thanh Hoang V, Lim J, Byon C, Min Park J (2017) Three-dimensional simulation of droplet dynamics in planar contraction microchannel. *Chem Eng Sci* 176:59–65
- Theisen E, Vogel M, Lopez C, Hirska A, Steen P (2007) Capillary dynamics of coupled spherical-cap droplets. *J Fluid Mech* 580:495–505
- To HD, Scheuermann A, Galindo-Torres SA (2015) Probability of transportation of loose particles in suffusion assessment by self-filtration criteria. *J Geotech Geoenviron Eng* 142:04015078
- Tomaiuolo G, Simeone M, Martinelli V, Rotoli B, Guido S (2009) Red blood cell deformation in microconfined flow. *Soft Matter* 5:3736–3740
- Tomita M et al (1999) E-CELL: software environment for whole-cell simulation. *Bioinformatics* 15:72–84
- Toose EM, Geurts BJ, Kuerten JGM (1999) A 2D boundary element method for simulating the deformation of axisymmetric compound non-Newtonian drops. *Int J Numer Meth Fluids* 30:653–674
- Tsai T, Miksis MJ (1994) Dynamics of a drop in a constricted capillary tube. *J Fluid Mech* 274:197–217
- Tsai C-HD, Sakuma S, Arai F, Kaneko M (2014) A new dimensionless index for evaluating cell stiffness-based deformability in microchannel. *Biomed Eng IEEE Trans* 61:1187–1195
- Van Hirtum A, Wu B, Gao H, Luo XJEJoM-BF (2017) Constricted channel flow with different cross-section shapes. *Eur J Mech-B/Fluids* 63:1–8
- Vazquez RM et al (2015) An optofluidic constriction chip for monitoring metastatic potential and drug response of cancer cells. *Integr Biol* 7:477–484
- Vogel MJ, Ehrhard P, Steen PH (2005) The electroosmotic droplet switch: countering capillarity with electrokinetics. *Proc Natl Acad Sci* 102:11974–11979
- Wang W, Huang Y, Grujicic M, Chrisey DB (2008) Study of impact-induced mechanical effects in cell direct writing using smooth particle hydrodynamic method. *J Manuf Sci Eng* 130:021012
- Watson KE, Dovi WF, Conhaim RL (2012) Evidence for active control of perfusion within lung microvessels. *J Appl Physiol* 112:48–53
- Wetzel ED, Tucker CL (2001) Droplet deformation in dispersions with unequal viscosities and zero interfacial tension. *J Fluid Mech* 426:199–228
- Wörner M (2012) Numerical modeling of multiphase flows in microfluidics and micro process engineering: a review of methods and applications. *Microfluid Nanofluid* 12:841–886
- Wu T, Feng JJ (2013) Simulation of malaria-infected red blood cells in microfluidic channels: passage and blockage. *Biomicrofluidics* 7:044115
- Wu T, Guo Q, Ma H, Feng JJ (2015) The critical pressure for driving a red blood cell through a contracting microfluidic channel. *Theor Appl Mech Lett* 5:227–230
- Wyss HM (2015) Cell mechanics: combining speed with precision. *Biophys J* 109:1997
- Xiao L, Liu Y, Chen S, Fu B (2016) Numerical simulation of a single cell passing through a narrow slit. *Biomech Model Mechanobiol* 15:1655–1667
- Xie Y et al (2016) Probing cell deformability via acoustically actuated bubbles. *Small* 12:902–910
- Xu J, Attinger D (2008) Drop on demand in a microfluidic chip. *J Micromech Microeng* 18:065020
- Xu K, Zhu P, Huh C, Balhoff MT (2015) Microfluidic investigation of nanoparticles' role in mobilizing trapped oil droplets in porous media. *Langmuir* 31:13673–13679
- Xu B et al (2017) Arch-like microsifters with multi-modal and clogging-improved filtering functions by using femtosecond laser multifocal parallel microfabrication. *Opt Express* 25:16739–16753
- Xue C, Wang J, Zhao Y, Chen D, Yue W, Chen J (2015) Constriction channel based single-cell mechanical property characterization. *Micromachines* 6:1794–1804
- Yap B, Kamm RD (2005) Mechanical deformation of neutrophils into narrow channels induces pseudopod projection and changes in biomechanical properties. *J Appl Physiol* 98:1930–1939
- Yazdani A, Karniadakis GE (2016) Sub-cellular modeling of platelet transport in blood flow through microchannels with constriction. *Soft Matter* 12:4339–4351
- Ye T, Phan-Thien N, Lim CT (2016) Particle-based simulations of red blood cells—a review. *J Biomech* 49:2255–2266
- Yoshino T, Tanaka T, Nakamura S, Negishi R, Shionoiri N, Hosokawa M, Matsunaga T (2017) Evaluation of cancer cell deformability by microcavity array. *Anal Biochem* 520:16–21
- Zeina K, Nabiollah K, Fazle H, Siva V (2017) Passage times and friction due to flow of confined cancer cells, drops, and deformable particles in a microfluidic channel. *Converg Sci Phys Oncol* 3:024001
- Zhang Z, Drapaca C (2016) A critical velocity of squeezing a droplet through a circular constriction: implications on ischemic stroke. *Bull Am Phys Soc* 61
- Zhang Z, Xu J, Hong B, Chen X (2014) The effects of 3D channel geometry on CTC passing pressure—towards deformability-based cancer cell separation. *Lab Chip* 14:2576–2584
- Zhang Y et al (2015a) Multiple stiffening effects of nanoscale knobs on human red blood cells infected with *Plasmodium falciparum* malaria parasite. *Proc Natl Acad Sci* 112:6068–6073
- Zhang Z, Chen X, Xu J (2015b) Entry effects of droplet in a micro confinement: Implications for deformation-based circulating tumor cell microfiltration. *Biomicrofluidics* 9:024108
- Zhang Z, Xu J, Chen X (2015c) Compound Droplet Modelling of Circulating Tumor Cell Microfiltration. Paper presented at the

- ASME 2015 international mechanical engineering congress and exposition
- Zhang X, Chen X, Tan H (2017a) On the thin-film-dominated passing pressure of cancer cell squeezing through a microfluidic CTC chip. *Microfluid Nanofluid* 21:146
- Zhang Z, Drapaca C, Chen X, Xu J (2017b) Droplet squeezing through a narrow constriction: minimum impulse and critical velocity. *Phys Fluids* 29:072102
- Zhang X, Hashem MA, Chen X, Tan H (2018) On passing a non-Newtonian circulating tumor cell (CTC) through a deformation-based microfluidic chip. *Theor Comput Fluid Dyn*. <https://doi.org/10.1007/s00162-018-0475-z>
- Zhao Y et al (2015) Simultaneous characterization of instantaneous Young's modulus and specific membrane capacitance of single cells using a microfluidic system. *Sensors* 15:2763–2773
- Zhao Y et al (2016) Single-cell electrical phenotyping enabling the classification of mouse tumor samples. *Sci Rep* 6:19487
- Zhao C, Ma W, Yu X, Su H, Zhang Z, Zohar Y, Lee Y-K (2017) The capillary number effect on cell viability in Microfluidic Elasto-Filtration devices for viable circulating tumor cell isolation. In: Solid-state sensors, actuators and microsystems (TRANSDUCERS), 2017 19th international conference on (2017). IEEE, pp 488–491
- Zheng Y, Shojaei-Baghini E, Azad A, Wang C, Sun Y (2012) High-throughput biophysical measurement of human red blood cells. *Lab Chip* 12:2560–2567
- Zhou C, Yue P, Feng JJ (2006) Formation of simple and compound drops in microfluidic devices. *Phys Fluids* 18:092105
- Zhou C, Yue P, Feng JJ (2007) Simulation of neutrophil deformation and transport in capillaries using newtonian and viscoelastic drop models. *Ann Biomed Eng* 35:766–780
- Zhou C, Yue P, Feng JJ (2008) Deformation of a compound drop through a contraction in a pressure-driven pipe flow. *Int J Multiph Flow* 34:102–109
- Zinchenko AZ, Davis RH (2006) A boundary-integral study of a drop squeezing through interparticle constrictions. *J Fluid Mech* 564:227–266
- Zinchenko AZ, Davis RH (2008) Squeezing of a periodic emulsion through a cubic lattice of spheres. *Phys Fluids* 20:040803
- Zinchenko AZ, Davis RH (2017) Motion of deformable drops through porous media. *Annu Rev Fluid Mech* 49:71–90
- Zolfaghari H, Izbassarov D, Muradoglu M (2017) Simulations of viscoelastic two-phase flows in complex geometries. *Comput Fluids* 156:548–561

Publisher's Note Springer Nature remains neutral with regard to jurisdictional claims in published maps and institutional affiliations.